CHEMISTRY
A EUROPEAN JOURNAL

DOI: 10.1002/chem.200600449

Supramolecular Self-Organization of "Janus-like" Diblock Codendrimers: Synthesis, Thermal Behavior, and Phase Structure Modeling

Izabela Bury, Benoît Heinrich, Cyril Bourgogne, Daniel Guillon, and Bertrand Donnio*[a]

Abstract: We report on the design and synthesis of three series of segmented amphiphilic block codendrimers, and on their self-organizing behavior in liquid-crystalline mesophases. Connecting two prefunctionalized monodendrons, each differing in their chemical constitution and generation number, yielded these diblock supermolecules. One wedge of the codendrimer was made hydrophobic, and is based on a branched poly(benzyl ether) monodendron functionalized at the periphery by lipophilic aliphatic fragments (also known as Percec dendrons). The other segment was made hydrophilic by the grafting of hydroxyl-containing moieties onto the focal functions of the former dendrons. Both types of dendrons were prepared independently by convergent methods and then joined in the ultimate stage of the synthetic procedure by cross-coupling reactions. In this way, the proportion of the dendritic blocks was varied independently to allow control of the hydrophilic/hydrophobic balance (HHB), the hydrogen-bonding ability, and consequently the capacity to tune the mesomorphic properties of the resulting "superamphiphiles" was anticipated. Essentially all the dendritic compounds display a thermotropic mesomorphism directly at or near room temperature as determined by using X-ray diffraction, polarized optical microscopy, and differential scanning calorimetry. The nature and the supramolecular organization of the mesophases, namely columnar and cubic phases, are correlated to the size of the respective block monodendrons and the chemical structures of the dendromesogens. The molecular organization within the cubic phases can be geometrically described and well understood by the space-filling polyhedron model.

Keywords: dendrimers · liquid crystals · mesophases · self-assembly · X-ray diffraction

Introduction

The dendritic pattern is one of the most pervasive, prolific, and influential natural topologies that can be observed on earth on all scales (from km to nm) and in both the inert and the living worlds. This hyperbranched architecture has reached an unrivalled level of perfection and one can speculate that such an evolution has provided maximum interfaces for efficient contacts and interactions, as well as for optimum information collection, transport, and distribution. The main inspiration for the conception and the synthesis of such aesthetically challenging architectures has been driven by the need to mimic the macroscopically ordered branching networks and to convey their functions at the molecular level.[1] Indeed, it is now admitted that artificial dendritic supermolecules offer unique functionalities and performances in various areas of science.[2] Now, the study of such systems has expanded, and has been developed at the interfaces of chemistry, physics, biology, and mathematics. This expansion has been motivated by the use of such complex and well-de-

[a] Dr. I. Bury, Dr. B. Heinrich, Dr. C. Bourgogne, Dr. D. Guillon, Dr. B. Donnio
Institut de Physique et Chimie des Matériaux de Strasbourg - IPCMS
Groupe des Matériaux Organiques - GMO
UMR 7504 - CNRS/Université Louis Pasteur
23, rue du Loess, BP 43, 67034 Strasbourg Cedex 2 (France)
Fax: (+33) 388-107-246
E-mail: bdonnio@ipcms.u-strasbg.fr

Supporting information for this article is available on the WWW under http://www.chemeurj.org/ or from the author. It contains experimental techniques, representative POM pictures and DSC traces, a phase diagram, a table (Table S1) gathering the results of XRD and DSC investigations, a table with the thermal behavior of the precursory dendrons (Table S2), a table of DSC and TGA data of the final dendrimers (Table S3), the XRD characterization of all the samples, snapshots of the packing of the dendrimers exhibiting a Col_h phase, figures showing details of the bond framework of clathrates and packing of polyhedrons, and the general synthetic procedures of the final dendrimers and intermediates along with the appropriate analytical characterization (^1H and ^{13}C NMR spectroscopy; HRMS-FAB and MALDI-TOF mass spectrometry, elemental microanalysis).

fined architectures, with a high degree of branching and multivalency, as scaffolds in organic-based materials (photonics, nanoarrays, ceramics, and molecular electronics),[2,3] in chemistry at surfaces and interfaces,[4] in nanoscaled organic–inorganic hybrids,[5] and in imaging, therapeutics, and biomimetics for specific biological functions (catalysis, magnetic resonance imaging (MRI), virus and proteins mimicking and/or recognition, gene transfection, and drug delivery).[2,3,6]

Through the adjustment of perfectly controlled and sequential reiterative synthetic processes, the chemistry of dendrimers has led to the most impressive developments and rapidly expanding areas of current chemistry.[2,3,7] These supermolecules can be obtained with a narrow molecular-weight distribution, and the ultimate molecular architecture can be accurately controlled (modulation of the molecular size, conformation, and shape) by the intrinsic critical molecular parameters, such as the multiplicity of branching (N_B), the length of the branches, the peripheral groups, the connectivity of the focal core (N_C), and the geometrical growth rate (the number of generation, N_G).[8] However, predictions by de Gennes and Hervet showed that the starburst growth was not infinite and that beyond a certain generation (which depends on these critical parameters), the branching is no longer regular and perfect due to steric hindrance.[9] This effect, known as the starburst dense packing, yields proteus-like structures reminiscent of "unimolecular cells" to which an apparent surface is associated.

Another interesting peculiarity of these supermolecules resides in the generation of periodically ordered, self-organized nano-[4c,d] and mesostructures,[10] where dendrimers and dendrons proved particularly versatile candidates for such uses and applications. The first liquid-crystalline dendrimers (LCDs) to be reported were obtained by simply incorporating mesogenic groups within a hyperbranched dendritic scaffold by random polymerization of an appropriate difunctionalized mesogenic monomer:[11c–f] such hyperbranched polymers,[12] a name used in preference to dendrimers, are characterized by randomly branched structures with a high degree of branching and broad molecular-weight distributions.[2,3,13] In contrast, the field of monodisperse LCDs has expanded more rapidly as evidenced by the development of many new structures able to self-assemble into periodic nanoarrays, including supramolecular dendromesogens,[14] shape-persistent systems,[15] fullerodendrimers,[16] and end-group (side-on and end-on branching topologies)[10] and main-chain (willowlike[17] and octopus[18]) LCDs. These dendrimers are thus representatives of an important class of mesomorphic materials, showing interesting potential uses and promise in various areas of materials science as new functional materials. LCDs also represent an interesting framework where mesomorphism can be easily modulated by very subtle structural modifications.[16,18,19]

Inspired by the beauty of such an architecture, and by the fundamental systematic study on supramolecular dendromesogens carried out by Percec et al.,[14] we designed amphiphilic diblock codendrimers (compounds **1**–**6**). The two compartments of the dendrimers have a different chemical nature and affinity, with the hope of producing original, large, and controlled nanosized self-assemblies. The concept of amphiphilicity in synthetic dendrimers is quite recent and has been successfully used, for example, to obtain unimolecular micelles for drug encapsulation and transport,[20] to mimic the aggregation of globular proteins,[21] or in therapeutic applications for their recognition ability towards protein receptors or biomedical materials.[6,22] Such amphiphilic dendrimers also have potential use as catalysts and phase-transfer agents for organic reactions in aqueous solutions.[23] Film formation was reported for surface-block dendrimers,[24] but as far as we are aware, the study of such liquid-crystalline systems as building blocks for self-ordered mesostructures has not yet been addressed.[25]

In this paper, we report on the synthesis and the self-assembling behavior of a broad library of compounds comprising 19 new amphiphilic codendrimers of the Janus type.[26] Various structural parameters were selectively modified in order to establish relationships between the molecular structure (control of the hydrophilic/hydrophobic balance (HHB) and hydrogen-bonding ability) and the self-organization properties for forming liquid-crystalline phases. These parameters include the generation numbers of both the hydrophobic ($N_G=1$ (G^1), 2 (G^2), and 3 (G^3)) and hydrophilic ($N_G=1$ (G^1) and 2 (G^2)) parts, which were changed independently, and the terminal chain number and substitution (compounds **1**–**6**). The thermotropic mesomorphism, as well as the nature of the self-organization of these surface-block dendrimers, are discussed on the basis of the chemical structures and polyhedral space-filling models.[27]

Results and Discussion

Synthesis: The lipophilic monodendrons were prepared by following the convergent synthetic procedure described by Percec.[14] The procedure involved repetitive chemical sequences such as the protection of the focal acid function into an ester function, the etherification of the peripheral hydroxy groups, and the transformation of the ester into either the acid (hydrolysis) or the benzyl alcohol (reduction) parent compounds (Scheme 3, discussed below). As for the hydrophilic part, the free hydroxy functions were protected by selective groups to avoid synthetic problems, and then used as such for the construction of the next generation (Scheme 1). The final block codendrimers were obtained by the cross-coupling of the various generations of poly(benzyl ether) acid and/or benzylic alcohol derivatives with the first and second generations of hydrophilic building blocks, respectively, immediately followed by the removal of the protecting groups, as shown in Scheme 4, below. Such a cross-synthesis allowed for a large number of compounds to be obtained rather rapidly, with an important reduction of elementary steps.

The delicate step for the construction of the diblock codendrimers was the synthesis of the hydrophilic lobes, as a

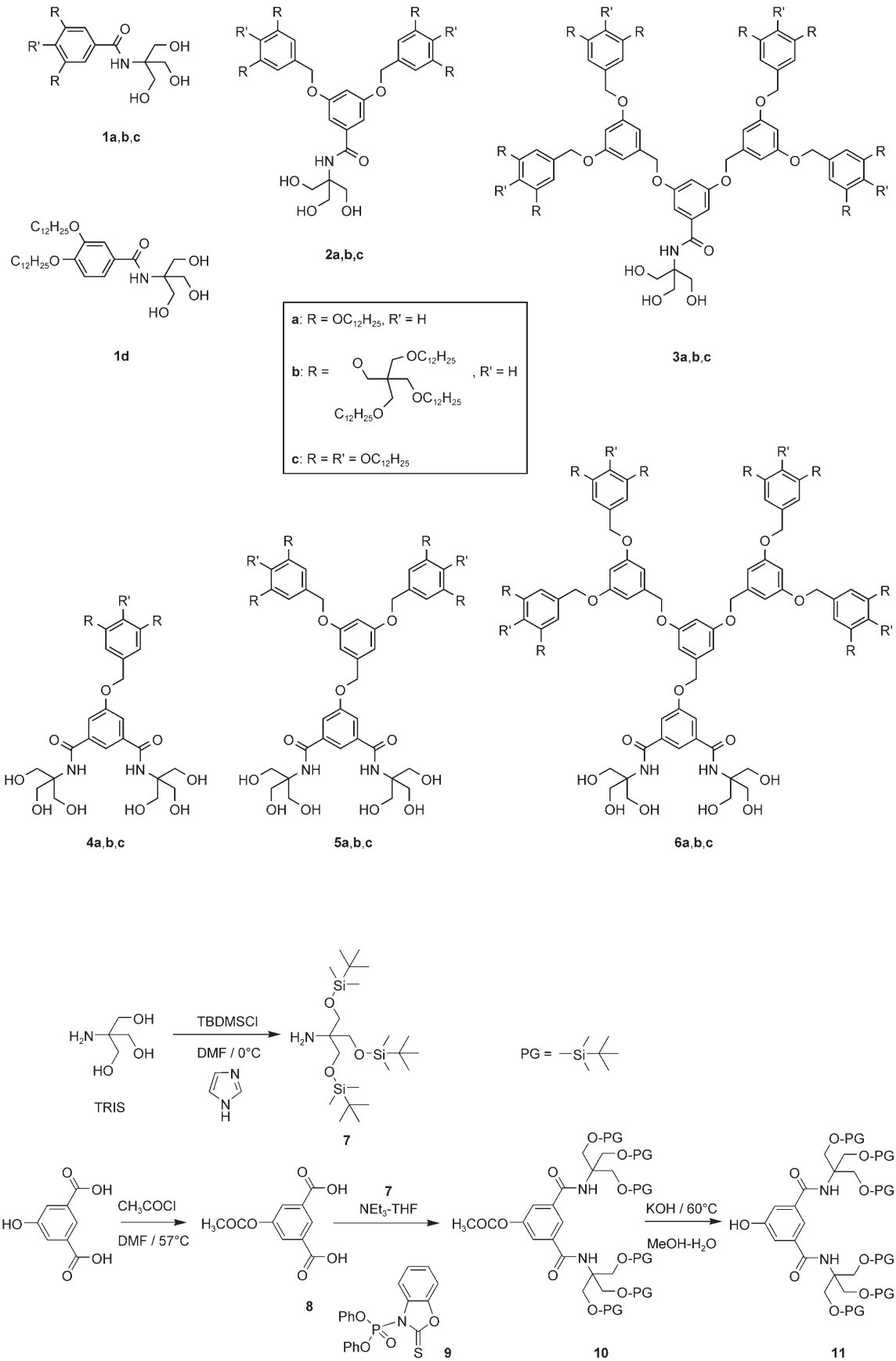

Scheme 1. Preparation of the precursory hydrophilic building blocks.

good compromise had to be found between a facile and selective method for the protection of the hydroxyl functions of tris(hydroxymethyl)aminomethane (TRIS) and a specific and efficient procedure for the removal of the protecting groups. *t*-Butyldimethylsilyl chloride (TBDMSCl) appeared to be the most suitable protecting agent in this case,[28] firstly because it quantitatively reacts with TRIS under slightly basic conditions (Scheme 1), and secondly, because it is easily removed with tetrabutylammonium fluoride (TBAF) at the ultimate stage of the synthesis without damaging the rest of the molecule (Scheme 4, below).

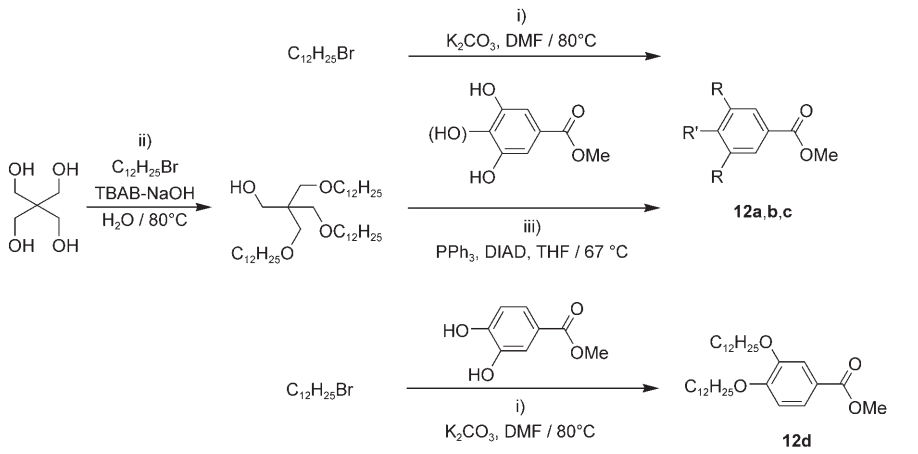

Scheme 2. Preparation of the peripheral blocks (**a**: $R=OC_{12}H_{25}$, $R'=H$; **b**: $R=OCH_2C(CH_2OC_{12}H_{25})_3$, $R'=H$; **c**: $R=R'=OC_{12}H_{25}$). TBAB = tetrabutylammonium bromide; DIAD = diisopropylazodicarboxylate.

Preparation of the precursory hydrophilic lobes of the first and second generation: As mentioned, the key step for the preparation of the hydrophilic parts consisted of the protection of the free hydroxyl functions of TRIS, which was achieved by the use of TBDMSCl under slightly basic conditions, to form the silylated derivative **7** (Scheme 1).[28] Prior to the double condensation reaction to form **10**, the isophthalic acid was transformed into its acetylated derivative, **8**, to avoid side reactions. This reaction was carried out in the presence of the condensing agent diphenyl(2,3-dihydro-2-thioxo-3-benzoxazolyl)phosphonate (**9**), successfully used in amidation reaction of polyamines.[29] Finally, the careful hydrolysis of **10** led to the precursory second-generation hydrophilic building block **11** with the six protected hydroxy groups (Scheme 1).

Preparation of the terminal functional groups of the hydrophobic monodendrons: For the surface functionality, the number and position of terminal chains (two or three aliphatic chains per final group **a**, **c**, and **d**) or the nature of the R group attached to methyl 3,5-dihydroxybenzoate (series **b**) were changed in order to explore the effect of congestion on the mesomorphic properties. Compounds **12a** and **12c** were obtained directly by a straightforward nucleophilic substitution of the reactive hydroxyl groups of the appropriate methyl benzoate with dodecylbromide (step (i) in Scheme 2), whereas **12b** with the bulkier trialkoxy pentaerythritol moiety was obtained in two steps (steps (ii) and (iii) in Scheme 2). The first step consisted of the alkylation of pentaerythritol with saturated primary alkyl bromides under a catalyzed phase-transfer procedure similar to that applied by Nouguier and Mchich,[30] followed by the grafting of the modified pentaerythritol moiety to methyl 3,5-dihydroxybenzoate under Mitsunobu reaction conditions.[31] Only the minidendrimer **12d** with *meta*,*para* chain substitution was synthesized for this study, and was prepared as **12a** and **12c** (Scheme 2, step (i)).

Preparation of hydrophobic dendritic parts of first, second, and third generation: Depending on the nature of the final dendrimers, that is, first (**1**–**3**) or second (**4**–**6**) hydrophilic generation, or on the terminal function (**a** systems: $R=OC_{12}H_{25}$, $R'=H$; **b** systems: $R=OCH_2C(CH_2OC_{12}H_{25})_3$, $R'=H$; **c** systems: $R=R'=OC_{12}H_{25}$), two subclasses of monodendrons from the first (G^1) to the third (G^3) generation, based on the AB_2 and AB_3 building block (methyl 3,5-dihydroxybenzoate and methyl 3,4,5-trihydroxybenzoate, respectively) were prepared, namely, the alcohol- (G^n-CH_2OH) and acid-based (G^n-CO_2H) monodendrons (Scheme 3). Thus, **13** (G^1-CO_2H), **14** (G^1-CH_2OH), **16** (G^2-CO_2H), **17** (G^2-CH_2OH), **19** (G^3-CO_2H), and **20** (G^3-CH_2OH) were prepared in cascade by using a convergent method (Scheme 3). The active first-generation dendrons of the benzyl ether type (**14**) were prepared by the reduction of the ester derivatives (**12**) with $LiAlH_4$. Then, the subsequent grafting of these benzylic alcohols to methyl 3,5-dihydroxybenzoate by Mitsunobu etherification led to the second generation dendrons of the ester type (**15a**, **15b**). In this case, the Mitsunobu method was preferred to the Williamson etherification as it saves the step of the conversion of the benzylic alcohol into its corresponding benzyl halide derivative. This process was then repeated for the next generation with the reduction of **15** into **17**, followed by the grafting of **17** to methyl 3,5-dihydroxybenzoate to yield the esters **18**. The ester dendron **15c** could not be prepared this way, and involved, prior to the etherification (Williamson type), the transformation of **14c** into its chloride derivative. The other series of active dendrons, that is, those with an acid group at the focal point (**13**, **16**, **19**), were prepared by hydrolysis of the corresponding esters (**12**, **15**, **18**).

Preparation of the block codendrimers: The dendrimers of the first series (**1**–**3**) with three hydroxyl groups were prepared from the precursory dendritic acids (**13**, **16**, **19**). The protected TRIS derivative **7** was prepared by an amide condensation reaction activated by **9**, followed by the removal of the protecting groups of the hydroxyl functions by using

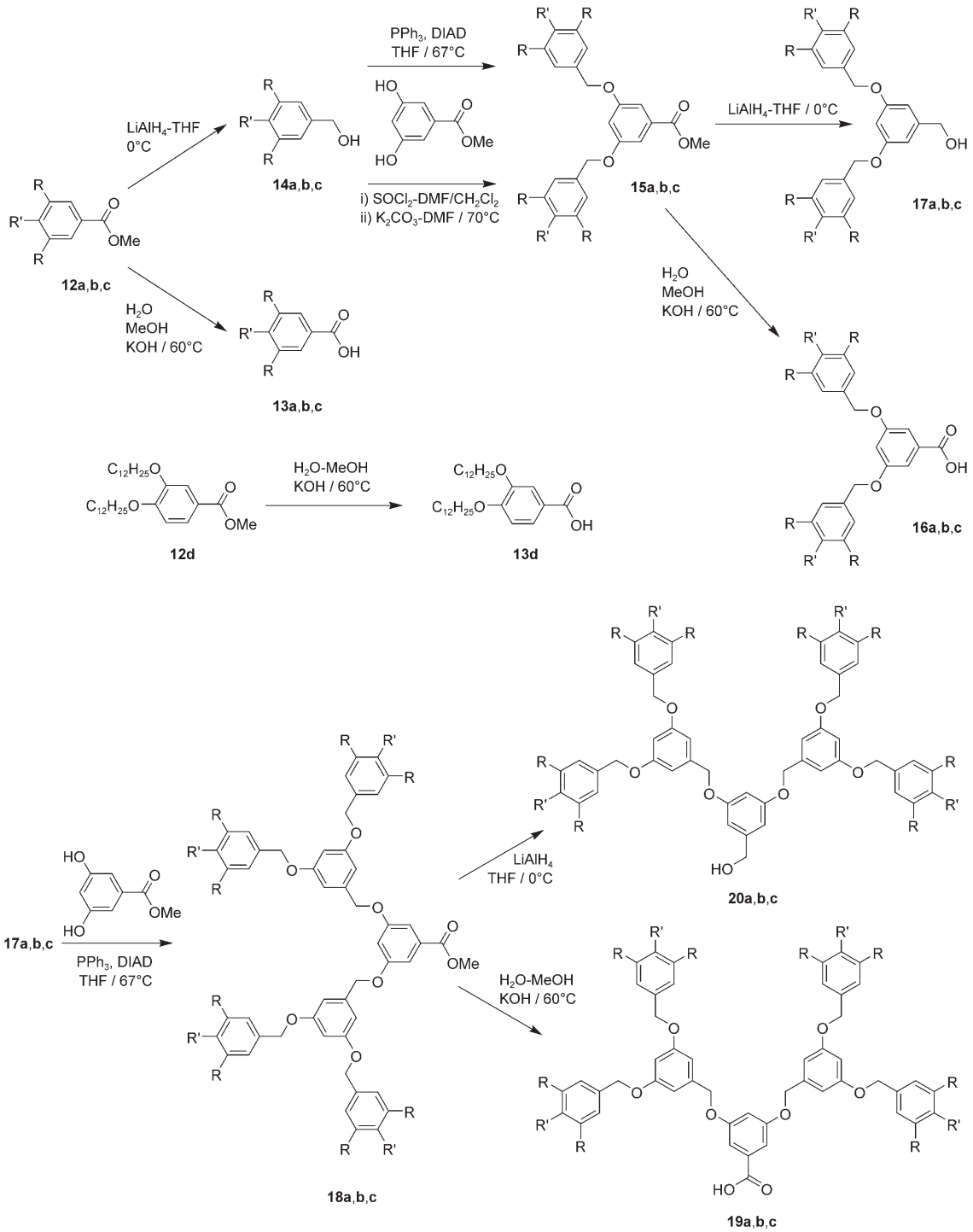

Scheme 3. Preparation of the hydrophobic monodendrons (**a**: R = $OC_{12}H_{25}$, R′ = H; **b**: R = $OCH_2C(CH_2OC_{12}H_{25})_3$, R′ = H; **c**: R = R′ = $OC_{12}H_{25}$).

TBAF (Scheme 4). The second series of block codendrimers (**4**–**6**, except **4c**) was synthesized by means of the direct Mitsunobu etherification of the isophthalic derivative **11** with the appropriate benzyl ether dendrimers (**14**, **17**, **20**), followed by the deprotection of the six hydroxyl groups (Scheme 4). Compound **4c** was prepared by direct etherification between the chloride derivative **14c′** and the alcohol **11** by using standard Williamson procedures (Scheme 4).

Structural characterization: The purity and characterization of the precursor dendritic derivatives and of all intermediary compounds were determined by using a combination of thin-layer chromatography (TLC) and ^1H and ^{13}C NMR spectroscopy, in addition to elemental analysis and matrix-assisted laser desorption/ionization time-of-flight mass spectroscopy (MALDI-TOF MS) for the final dendrimers (see the Supporting Information). The results were, in all cases,

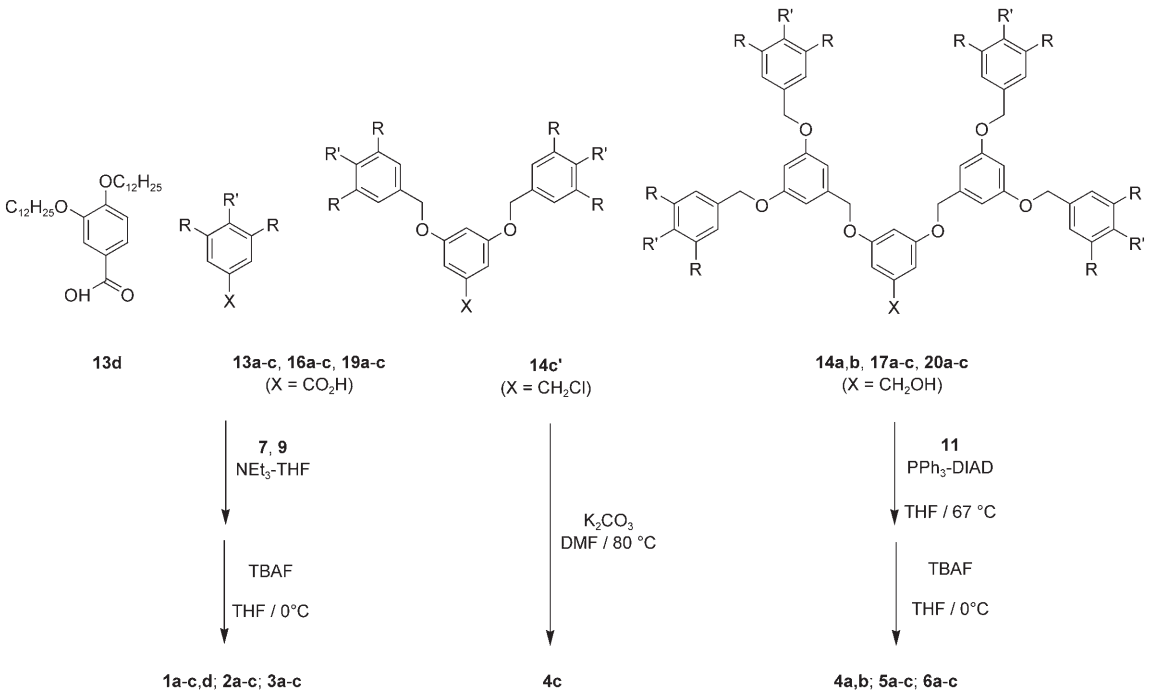

Scheme 4. Preparation of the block codendrimers (**a**: R = $OC_{12}H_{25}$, R′ = H; **b**: R = $OCH_2C(CH_2OC_{12}H_{25})_3$, R′ = H; **c**: R = R′ = $OC_{12}H_{25}$).

in good agreement with the proposed structures. The absolute molecular weights were given by MALDI-TOF MS, which showed the correct molecular peaks with additional lower-mass fragments, which did not correspond to intermediate compounds, in small amounts.

Mesomorphic behavior: The thermal behavior of the precursory monodendrons and of the dendrimers was investigated by four complementary techniques: polarized optical microscopy (POM), thermogravimetric analysis (TGA), differential scanning calorimetry (DSC), and small-angle X-ray diffraction (XRD).

Optical and thermal studies by using POM, DSC, and TGA: The homologous monodendrons with the same arborescent-like architecture, but with the terminal chains substitution in the 3,4-[14e] (compounds of type **1**, **2**, and **3** of series **d**) and 3,4,5-[14h]positions (**1**, **2**, and **3** of series **c**), displayed mesomorphic properties from the second generation for the former type, or from the third generation onwards for the latter systems (see Table S2 in the Supporting Information). However, none of the precursory hydrophobic monodendrons of the first, second, and third generations with substitution in the 3,5-positions, bearing an ester (**12**, **15**, **18**), an alcohol (**14**, **17**, **20**), or an acid (**13**, **16**, 1**9**) focal function, were found to be mesomorphic. These compounds melted directly into an isotropic liquid or were liquids at or near room temperature. The absence of mesomorphism is likely associated with the chain-substitution pattern (3,5 here) of the terminal benzene rings, at least for the first series with a linear dodecyloxy chain (series **a**). This substitution pattern disfavors the induction of mesomorphism, as already observed in other mesogenic systems such as polycatenars[32] or dendrimers.[18] As for the intermediate OH-capped codendrimers, most of them were also deprived of mesomorphism (obtained as viscous oils or as sticky glues), and were not analyzed further. In contrast, liquid-crystalline behavior was induced in essentially all of the amphiphilic codendrimers, as deduced from observation of the textures under cross polars in a polarized-light microscope. In some cases, homogeneous, characteristic birefringent and fluid optical textures (see the Supporting Information) that coalesced on increasing the temperature were observed. In other cases, no texture could be observed; just the formation of large, black (optically isotropic) viscous areas. However, applying some pressure with a spatula on the cover slip induced luminescent flashes, which immediately disappeared when the pressure was released. This feature, along with the careful observation of a preparation without a cover slip, which showed the faceting of air bubbles[33] (polygonal forms) trapped within the viscous phase, suggested the existence of a cubic structure. However, no precise mesophase assignment could be deduced from this technique only.

Partly confirming the results of the microscopic observations, several transitions were also detected by using DSC through a change in enthalpy at the temperatures close to those determined by using POM. The thermal stability was also checked by thermogravimetric analysis and indicated that extensive decomposition (>5 wt%) occurred at or in the vicinity of the clearing temperature. Thus, in order to

avoid decomposition and to obtain utilizable DSC traces, the experiments were carried out according to a specific protocol (see the Supporting Information).

Structural investigation of the mesophases by using small-angle X-ray diffraction: Identification and unequivocal mesophases assignment was eventually achieved by using small-angle X-ray diffraction on powder samples. The liquid-crystalline nature of the materials was confirmed by the presence of several sharp and intense reflections in the small-angle region, which allowed, in all cases, the determination of the mesophase symmetry, and of a broad scattering halo located at around 4.5 Å, characteristic of the liquidlike order of the molten aliphatic chains. A good agreement between the transition temperatures determined by using XRD, POM, and DSC analyses was generally found. The results of these investigations and the unit-cell parameters of all the mesophases for all the compounds are gathered in Table 1 (see also Table S1 in the Supporting Information).

Triols: Among the dendritic compounds **1a**, **2a**, and **3a**, bearing two terminal linear chains in the 3- and 5-positions of the benzyl end groups and three hydroxyl groups, only those of the second and third generation were directly mesomorphic at room temperature. They exhibit either a hexagonal columnar phase (**2a**: Col_h 85 I) or a cubic phase (**3a**: Cub 69 I), with the lowest generation member of the series present in a crystalline state before melting into an isotropic liquid (**1a**: Cr 93 I). The transition temperature to the isotropic liquid was found to decrease along with the increasing generation number from 93 to 85 to 69 °C for **1a**, **2a**, and **3a** respectively, emphasizing the strong destabilizing effect of the molten chains and the role of the hydrophobic/hydrophilic balance (HHB). The hexagonal two-dimensional lattice of the mesophase of **2a** was deduced from the three sharp, small-angle reflections, for which the reciprocal spacings were in the ratio 1, $\sqrt{3}$, and $\sqrt{4}$, and indexed in a hexagonal plane lattice as $(hk)=(10)$, (11), and (20), respectively (Figure 1a).

The cubic structure of **3a** was deduced from a set of six sharp small-angle reflections for which the reciprocal spacings were in the ratios $\sqrt{4}$, $\sqrt{5}$, $\sqrt{6}$, $\sqrt{8}$, $\sqrt{14}$, and $\sqrt{16}$. These reflections were indexed as (200), (210), (211), (220), (321), and (400) in a primitive cubic cell on the basis of the following analysis (Figure 1b, Table 1). For a body-centered cubic lattice (I type), the considered sequence in this case would have been: $\sqrt{8}$, $\sqrt{10}$, $\sqrt{12}$, $\sqrt{16}$, $\sqrt{28}$, and $\sqrt{32}$ (the general condition for the (hkl) reflections is $h+k+l=2n$). Because the ratio $\sqrt{28}$ is forbidden, the I-type Bravais lattice is therefore excluded. Among the allowed face-centered cubic lattices (F type), most are very unlikely because too many small-angle reflections are missing, and these absences are not explained by the reflection conditions; only two face-centered groups may be retained, namely $F\bar{4}3c$ and $Fm\bar{3}c$. As far as the 15 primitive cubic space groups (P type) are concerned, several could be immediately disregarded due to the presence of forbidden reflections such as the (210) reflex, excluding the $Pn\bar{3}$, $Pn\bar{3}n$, and $Pn\bar{3}m$ space groups, and the (200) reflex, eliminating the $P4_332$ and $P4_132$ space groups. Amongst the ten remaining primitive and retained face-centered groups, the most probable groups are $Pm\bar{3}n$, $P\bar{4}3n$, and $Pa\bar{3}$ (the least probable ones being $P2_13$, $P4_232$, $F\bar{4}3c$, $Fm\bar{3}c$, $P23$, $Pm\bar{3}$, $P432$, $P\bar{4}3\,m$, and $Pm\bar{3}m$). None of the space groups retained in this list have

Table 1. Thermal behavior of the amphiphilic block codendrimers.

Compd	Transition temperatures [°C][a]	Mesophase parameters (at T [°C])[b]
1a	Cr 93 I	–
2a	G −28 Col_h-*p6mm* 85 I	$D=39.3$ Å, $S=1\,340$ Å^2 ($T=50$)
3a	G 14 Cub-$Pm\bar{3}n$ 69 I	$a=81.5$ Å, $V_{cub}=541\,345$ Å^3 ($T=50$)
4a	Cr 80 LamCr 115 Col_h-*p6mm* 173 I	$d=32.0$ Å, $A_M=46.2$ Å^2 ($T=90$) $D=45.7$ Å, $S=1\,810$ Å^2 ($T=130$)
5a	Cr 52 LamCr 92 Col_h-*p6mm* 163 I	$d=48.4$ Å, $A_M=50.0$ Å^2 ($T=50$) $D=49.8$ Å, $S=2\,150$ Å^2 ($T=100$)
6a	G 28 Cub-$Im\bar{3}m$ 143 decomp	$a=63.3$ Å, $V_{cub}=253\,060$ Å^3 ($T=100$)
1b	liquid oil	–
2b	liquid oil	–
3b	liquid oil	–
4b	Cr −28 Cub-$Im\bar{3}m$ 172 I	$a=54.7$ Å, $V_{cub}=163\,670$ Å^3 ($T=100$)
5b	Cr −21 Cub-$Im\bar{3}m$ 129 I	$a=59.05$ Å, $V_{cub}=205\,900$ Å^3 ($T=50$)
6b	Cr −15 Cub-$Im\bar{3}m$ 42 I	–
1c	Cr 62 Col_h-*p6mm* 74 I	$D=40.1$ Å, $S=1\,395$ Å^2 ($T=50$)
2c	Cr_1 −7 Cr_2 20 Col_h-*p6mm* 125 decomp	$D=44.5$ Å, $S=1\,715$ Å^2 ($T=40$)
3c	Cr_1 −43 Cr_2 50 Cub-$Pm\bar{3}n$ 109 decomp	$a=82.9$ Å, $V_{cub}=569\,663$ Å^3 ($T=80$)
4c	Cr_1 −2 Cr_2 108 Col_h-*p6mm* 179 decomp	$D=50.35$ Å, $S=2\,195$ Å^2 ($T=140$)
5c	Cr_1 15 Cr_2 32 Col_h-*p6mm* 167 decomp	$D=54.15$ Å, $S=2\,540$ Å^2 ($T=100$)
6c	G −15 Cub-$Im\bar{3}m$ 153 decomp	$a=66.2$ Å, $V_{cub}=290\,064$ Å^3 ($T=100$)
1d	Cr 113 Col_h-*p6mm* 130 I	$D=47.1$ Å, $S=1\,925$ Å^2 ($T=60$)

[a] Cr, Cr_1, Cr_2 = crystalline phases; G = amorphous or partially crystallized solid phase; I = isotropic liquid; LamCr = lamellar crystalline phase; Col_h = hexagonal columnar phase; Cub = cubic phase; decomp: decomposition temperature. [b] d = lamellar periodicity; A_M = molecular area; D = lattice parameter of the Col_h phase; S = lattice area; a = lattice cubic phase parameter; $V_{cub}=a^3$ (volume of the cubic cell).

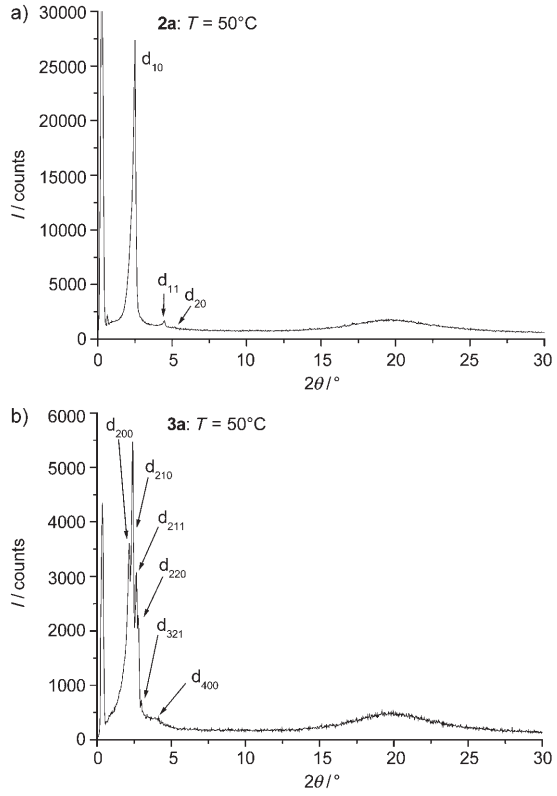

Figure 1. X-ray diffractograms of a) the Col_h phase of **2a** (*p6mm*) and b) the cubic phase of **3a** ($Pm\bar{3}n$).

yet been found for a liquid-crystalline cubic phase, except the $Pm\bar{3}n$ cubic space group (no. 223), though, none of them can be totally discarded.

The cubic mesophase occurs in a phase sequence $Col_h \rightarrow$ Cub on increasing the generation number while keeping the size of the polar lobe constant. Therefore, from packing considerations and in agreement with the molecular shape, the polar/apolar interface curvature becomes increasingly negative[34] along this sequence, suggesting that the three-dimensional cubic lattice of compound **3a** probably consists of discrete micellar aggregates with the polar parts forming the nucleus of the micelle, surrounded by the nonpolar chains (inverted micellar cubic phase) rather than the bicontinuous structure consisting of infinite interwoven networks. For lyotropic micellar cubic phases made of discrete aggregates (I_1, I_2), the group $Pm\bar{3}n$[35] is the most commonly encountered cubic space group along with the $Im\bar{3}m$, $Fm\bar{3}m$, and $Fd\bar{3}m$[36] groups. Recently, some of their thermotropic liquid-crystalline counterparts have been discovered, and only $Pm\bar{3}n$ and $Im\bar{3}m$ space groups have yet been found.[14b,37] With this in mind, and by analogy with those studies, the $Pm\bar{3}n$ cubic space group will be considered as the most probable for the symmetry of the cubic phase shown by this compound.

This trend was confirmed for the other closely related dendrimers of series **c** (aliphatic chains in the positions 3, 4 and 5 of the benzyl end groups) in that the same sequence was observed, except for the first homologue, which is mesomorphic. Thus, **1c**[38] and **2c** exhibit a Col_h phase (**1c**: Cr 62 Col_h 74 I; **2c**: Cr 20 Col_h 125 decomp), whereas **3c**, as **3a**, self-assembles into a cubic phase (**3c**: Cr 50 Cub 109 decomp). Despite the limited number of reflections present in the X-ray pattern of **3c** compared with that of **3a**, it was nevertheless possible to also assign the $Pm\bar{3}n$ symmetry to this cubic phase due to the strong similarity between the two diffractograms (the intensity distribution of the first reflections is exactly the same in both cases, indicating the same distribution of the electronic density, and thus the same symmetry; see the Supporting Information). Only one member of series **d** (aliphatic chains in the positions 3 and 4 of the benzyl end groups) was prepared, namely, the minidendrimer of the first-generation compound **1d**, which is also mesomorphic, and also shows a Col_h phase (**1d**: Cr 113 Col_h 130 I).

Such a trend in the phase sequence from columnar to micellar cubic phases observed with the generation growth was expected and is consistent with the results of Tschierske[37a,d,38,39] or Percec.[14,37c] Indeed, the increase of the hydrophobic part with respect to the hydrophilic block forces the molecules to change their overall shape from a two- to three-dimensional shape in order to optimize the interfacial curvature between the two parts, and to express the bipolar nature of these species. Consequently, due to microsegregation effects and geometric constraints, these dendrimers self-assemble into supramolecular dendrimers with well-defined shapes: infinite cylindrical micelles and/or discrete micellar aggregates, leading to the formation of the Col_h phase (self-organization of the columnar supramolecular dendrimers into a two-dimensional hexagonal lattice) and the cubic phase (self-organization of the supramolecular dendrimers into cubic lattices), respectively. The details of these organizations will be discussed in the next section.

Increasing the density of terminal aliphatic chains even more by the grafting of the bulkier tridodecyloxy pentaerythritol moieties in place of the dodecyloxy chains (compounds **1b**, **2b**, **3b**) led to the complete destruction of the mesomorphism; the three compounds were obtained as room-temperature isotropic oils. DSC investigations performed between 20 and −120 °C did not reveal any transition either. Such a pure liquidlike behavior was not expected, though the absence of mesomorphism is not fully surprising. The amphiphilic character is totally lost with such a large number of aliphatic chains because the tripodal polar part becomes meaningless compared with the volume of the aliphatic chains. The shapeless nature of the dendrimers probably inhibits the tendency of a periodic aggregation into any mesophase.

Hexols: All the members of the other series of dendrimers with the second dendritic generation hydrophilic lobe (six hydroxyl groups, compounds **4**, **5**, and **6**), were mesomorphic, exhibiting columnar hexagonal Col_h (**4a**, **5a**, **4c**, **5c**) and cubic phases (**6a**, **6c**) (Table 1). In addition, **4a** and **5a** exhibited a lower temperature semicrystalline phase with a

lamellar morphology, described as LamCr. In general, the mesomorphic temperature range was extended considerably when compared with that of the homologous dendrimers with three hydroxyl units, likely because it was connected to a more extended hydrogen-bonding network (stronger HHB). However, almost all the compounds started to decompose before reaching the isotropic liquid state. As for the compounds described above, the Col_h phase was deduced from the analysis of the X-ray diffractograms (see the Supporting Information), which showed three (**5a**) or four (**4a**) sharp small-angle reflections indexed to a two-dimensional hexagonal plane, accompanied by a broad diffuse scattering at 4.6 Å. Similar X-ray patterns were observed for **4c** and **5c**.

As for the cubic phase exhibited by **6a**, a set of twelve small-angle reflections (see Supporting Information), for which the reciprocal spacings were in the ratios 1, $\sqrt{2}$, $\sqrt{3}$, $\sqrt{4}$, $\sqrt{5}$, $\sqrt{6}$, $\sqrt{7}$, $\sqrt{9}$, $\sqrt{12}$, $\sqrt{13}$, $\sqrt{15}$, and $\sqrt{16}$, was observed. The presence of the reflections corresponding to the ratio $\sqrt{7}$ and $\sqrt{15}$ allows the immediate elimination of any primitive (*P*-Bravais type) and face-centered (*F*-Bravais type) space groups. Thus, for a body-centered cubic lattice (*I* type), the considered sequence in this case must be $\sqrt{2}$, $\sqrt{4}$, $\sqrt{6}$, $\sqrt{8}$, $\sqrt{10}$, $\sqrt{12}$, $\sqrt{14}$, $\sqrt{18}$, $\sqrt{24}$, $\sqrt{26}$, $\sqrt{30}$, and $\sqrt{32}$, and the reflections were indexed as (110), (200), (211), (220), (310), (222), (321), (411/330), (422), (431/510), (521), and (440). Amongst the ten centered groups, four can be eliminated due to the presence of forbidden reflections not allowed by the general conditions, that is, the groups $Ia\bar{3}$, $I4_132$, $I\bar{4}3d$, and $Ia\bar{3}d$. We are left with six groups with similar probabilities (they all have the same general conditions of extinction), which are $I23$, $I2_13$, $Im\bar{3}$, $I432$, $I\bar{4}3m$, and $Im\bar{3}m$. As above, by analogy with all known cubic space groups discovered, and particularly those found for thermotropic micellar cubic phases,[37] the one we will consider to be the most likely is the $Im\bar{3}m$ space group (no. 229). Here too, despite the limited number of reflections present in the X-ray pattern of **6c** relative to that of **6a**, it was nevertheless possible to assign the $Im\bar{3}m$ symmetry to this cubic phase due to the strong similarity between the two diffractograms (same intensity distribution of the first reflections).

Again, the cubic phase occurs in a phase sequence LamCr→Col_h→Cub as a function of the increasing generation of hydrophobic substituents. At first sight, this gradual change from a columnar to a micellar cubic structure was expected and in agreement with the results described by Percec.[14] However, due to the molecular structure of the first two members of the series **a** and **c**, and particularly that of **4a** and **4c**, the formation of a "classical" Col_h phase was quite surprising and unexpected. Indeed, for these samples, the cross section of the polar head is larger (**4a**, **4c**) or similar (**5a**, **5c**) relative to that of the lipophilic part ("reverse" flat, tapered conformation), a structural requirement a priori incompatible with the formation of inverted columnar phases.[34] By means of molecular modeling and molecular dynamics, an explanation of the structure of the Col_h phase is given and will be discussed below. In contrast, the cubic phase for **6a** and **6c** was totally expected. Interestingly, the space group for the cubic phase is different and changed upon the huge volume increase of the polar part from $Pm\bar{3}n$ to $Im\bar{3}m$, when compared with the analogous compounds of the **3** type.

Finally, the last three compounds (**4b**, **5b**, **6b**) bearing the bulky trifurcated chains all showed a cubic phase, from room temperature up to the clearing point, which decreased rapidly from 172 to 129 to 42 °C with increasing generation. For these compounds, the volume of the chains is already important right from the first generation (6, 12, and 24 chains for **4b**, **5b**, and **6b**, respectively) so that the conformational criteria required for self-assembly into micelles is reached even for the smallest member of the series. The cubic phase was deduced from the X-ray patterns for which three (**4b**) and four (**5b**) small-angle reflections were observed in the ratio 1, $\sqrt{2}$, $\sqrt{3}$, $\sqrt{4}$, and $\sqrt{5}$ (Figure 2). Unfortunately, **6b** could not be analyzed by means of X-ray diffraction because of some experimental difficulties such as its high viscosity and sticky character at room temperature. However, the existence of the cubic phase was proven by POM observations (see above). By analogy with **6a**, and the similarity of the diffractograms, the structure of these cubic phases is regarded as isomorphous, and thus, the reflections were indexed in the body-centered $Im\bar{3}m$ space group as (110), (200), (211), (220), and (310). These results were expected on the basis of the behavior of the preceding series. Here, though, the dendrimers likely adopt a conical shape right from the first generation due to the strong interfacial curvature, and have a strong amphiphilic character as the polar parts are important. These dendrimers then self-assemble into pseudospherical supramolecular micelles, which are located at the eight corners and in the center of the cubic lattice. The model of this organization will be discussed in the next section. The mesomorphic properties are summarized in Table 1 and in the phase diagram shown in the Supporting Information.

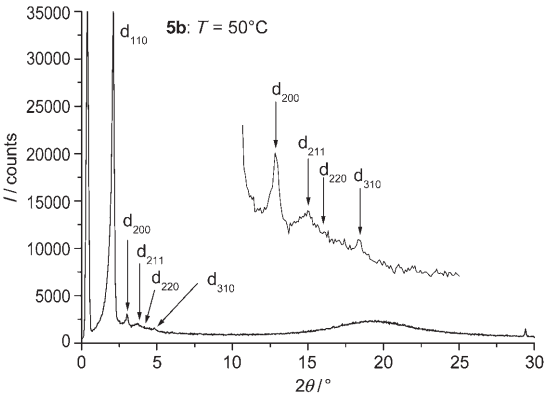

Figure 2. X-ray diffractogram of the cubic phase of **5b** ($Im\bar{3}m$).

Supramolecular organization and modeling

Columnar hexagonal phase (Col_h-p6mm): All the triol compounds of the first (**1c**, **1d**, except **1a**) and second generation (**2a**, **2c**) as well as four hexols of the first and second generation (**4a**, **4c**, **5a**, and **5c**) were found to exhibit a Col_h-*p6mm* phase. All differ by their polar/apolar ratio, that is, by the size of their respective constitutive lobes. Taking these structural differences into account within these series of mesogens, it was expected that their molecular organizations into the mesophase might slightly differ, and as such the specific molecular packing of each compound into the mesophase will be discussed separately hereafter.

As far as **2a** and **2c** are concerned, the structural requirement necessary to induce an inverted columnar phase (negative curvature of the interface, that is, when the apolar chains radiate out of the columnar spines) is satisfied. Indeed, the four or six side chains cover the periphery of the dendron from the wide end, whereas the narrow end is constituted of polar hydroxy groups. When the chains are molten, the mismatch at the polar/apolar interface is further enhanced, favoring the microsegregation of these tapered molecules into cylindrical structures (the number of chains being too small to drive the organization into micellar cubic structures). Thus, it is very likely that the dendrimers self-assemble in such a way that the polar apices segregate to form the polar columnar core of the cylindrical micelle, further stabilized by a dense and interlocked hydrogen-bonding network. The hydrophobic branches surround the wall of the inner columnar core (hydroxyl–dendritic interface), with the aliphatic chains radiating laterally.

The dimensions of these molecules in a flat conformation are fully compatible with the hexagonal lattice parameter, with the radius of the tapered molecule (equal in a first approximation to the height of the triangular mesogen) being close to half the intercolumnar distance, *D*. Knowing the molecular volume of **2a**, which can be estimated to be approximately 1990 Å^3 (at $T=50\,^\circ$C), it is found that three molecules (or molecular equivalents) completely fill a slice of column 4.5–4.6 Å thick. In order to pave (or fill) the hexagonal lattice efficiently, the molecules, which are radially oriented, are packed side-by-side to form a thick disclike slice as in a pizza.[14] As for **2c**, a slight expansion of the hexagonal lattice was observed when compared with that of **2a**, consistent with the extra volume required for the accommodation of two additional chains per dendron ($V_{mol}=2$ 590 Å^3 at $T=40\,^\circ$C). Using the same calculation, it is found that three molecules self-assemble into a supramolecular disc 4.6 Å thick with a cross section compatible with that of the hexagonal unit. In this respect, the packing of **2a** and **2c** into the Col_h phase is the same as that proposed by Percec for his dendromesogens, and is driven by the steric congestion, the amphiphilic character of the molecules (molecular recognition), and the formation of a dense hydrogen-bonding network.[14] This dense packing model of the dendrimers into columns was supported by molecular dynamics. A periodic molecular model for these two compounds was built from experimental X-ray data, though it was convenient to consider a slice thickness of 9.2 and 9.0 Å for **2a** and **2c**, respectively, and thus six molecules per defined slice (Table 2). The result of these calculations showed a good space filling of the available volume, as well as the enhancement of the microsegregation over the entire simulation experiment time, contributing to the cohesion of the structure. Snapshots of these experiments showing the excellent molecular packing of **2a** and **2c** in the Col_h phase are shown in the Supporting Information.

Similarly, the two minidendritic triols **1c** and **1d** and the dendritic hexol compounds, **4a**, **4c**, **5a**, and **5c** also form a Col_h phase, despite the fact that some of them do not possess a priori structural requirements to self-assemble into such phases (i.e., with an inverted structure). Indeed, the greater size of their polar parts with respect to their apolar parts should in principle favor the formation of normal phases (i.e., with a positive interfacial curvature). Therefore, self-organization into a columnar phase resembling the H_1 phase observed in lyotropic[40] and in some amphotropic[41] systems could not be immediately excluded. Recall that in such a normal phase, the polar heads of the molecules are directed outwards from the core to form a hydrophilic outer-wall interface, whereas the lipophilic fragments fill the internal core. In the case of the lyotropic systems, such an arrangement is even facilitated more as it occurs in the presence of a polar solvent like water. Under these conditions, the solvent contributes to the swelling of the polar part, to the dilution of the hydrogen-bonding network, to the smoothing of the interface by counterbalancing the geometric constraints, and to the fluidity of the system by filling the empty cavities. However, this normal arrangement seems very unfavorable in anhydrous materials and up to now only two examples of normal phases (Col_h and cubic phases) have been reported in thermotropic systems.[42] Indeed, if such an organization into normal columns was true here, the

Table 2. Parameters[a] of the Col_h phase of the dendrimers **1**, **2**, **4**, and **5**.

Compd	D [Å]	h [Å] (MD)	N	h [Å] (NV_{mol}/S)	ρ (MD)	Σ [Å^2] (Γ [Å])	a_{ch} [Å^2]
1c	40.1	9.375	10	9.437	1.007	1 310.9 (138.9)	44
1d	47.1	9.42	18	9.449	1.003	1 541.7 (163.2)	43
2a	39.3	9.2	6	8.923	0.970	1 214.7 (136.1)	51
2c	44.5	9.0	6	9.059	1.006	1 396.4 (154.15)	39
4a	45.7	6.75	8	6.719	0.995	1 063.7 (158.3)	66
4c	50.35	8.47	10	8.473	1.000	1 477.8 (174.4)	49
5a	49.8	9.0	8	9.326	1.036	1 608.8 (172.5)	50
5c	54.15	9.76	8	9.922	1.017	1 861.3 (187.6)	39

[a] D, h, N, ρ, Σ, and Γ are the intercolumnar distance, thickness of a columnar slice (repeating periodicity), number of molecules per such slice, density estimated by MD, interface of the hexagonal cell h-thick ($\Sigma=h.\Gamma$) area and perimeter ($\Gamma=6l=2\sqrt{3}D$) of these cells. a_{ch} = cross-sectional area of the terminal aliphatic chains calculated on the Wigner-Seitz cell walls.

honeycomb structure, which would be extended in the third direction and solidified by a dense hydrogen-bonding network, would not be compatible with the high fluidity of the mesophases observed by using POM. Consequently, the classical inverted model has thus been considered for the description of the molecular arrangement of these amphiphiles. It was therefore necessary to support this hypothesis by molecular dynamics (MD) in order to understand such a molecular organization within the Col_h phase.

Using the geometrical approach described above, it was found that a hexagonal cell, 4.5 Å thick, contains 5.35 molecules of **4a** ($D=45.7$ Å, $V_{mol}=1520$ Å^3 at $T=130$ °C). Considering the hypothesis of a mesophase based on supramolecular columns with a polar interior core, there is no effective possibility to arrange 5.35 of these mesogens in such a cell that respects both a perfect paving of the hexagonal two-dimensional lattice (with **4a** possessing only two aliphatic chains) and a good agreement between molecular and mesostructural dimensions. Indeed, the bulky polar fragment occupies a large volume not easily compensated for by the reduced number of aliphatic chains per molecule. A solution to this problem was given by computer modeling. The optimization of the geometry by molecular dynamics at 130 °C, the temperature at which the X-ray experiment was performed, led to a hexagonal lattice (with $D=45.7$ Å fixed before calculation) with a thickness of 13.5 Å and containing 16 molecules in the cell (these quantities correspond to the same ratio of 5.35 molecules per 4.5 Å-thick stratum, and thus to the same packing density). Comparing the molecular dimensions and the lattice size, the best compromise was found when the 16 molecules are placed into two strata of 6.75 Å thick, each stratum containing eight molecules arranged in such a way that they form a cylinder and occupy the available space homogeneously (Figure 3). In this simulation, the relative arrangement of the molecules is not random, adapting their shape in order for the polar segments to be localized in the central part of the discs, that is, in the interior of the column (Figure 3), to allow strong hydrogen-bonding interactions. The density ratio calculated at 130 °C, estimated from MD and XRD analyses (Table 2), was found to be very close to unity (0.995), and therefore supports this arrangement. The relative size of the region occupied by the polar parts is also rather large with respect to that filled by the aliphatic and aromatic parts, therefore suggesting here that the dominant driving force for mesophase formation is clearly the hydrogen-bonding interactions between the hydroxy groups. These interactions are necessary to stabilize the columnar polar spine, the chains forming the infinite continuum.

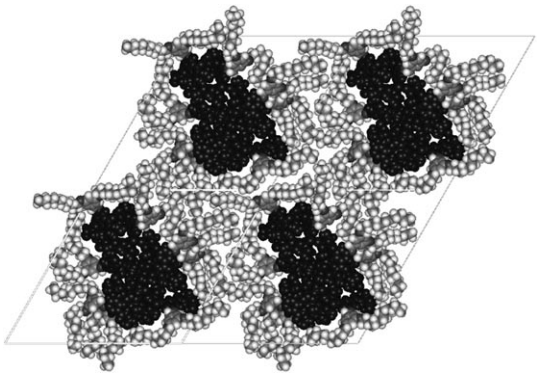

Figure 3. Snapshot showing the organization of **4a** in the Col_h phase (black = polar central core). Only one layer (6.75 Å) is represented. The apparent empty zones are actually filled by neighboring layers.

Similarly, we also resorted to molecular dynamics to understand the packing of **5a** in the Col_h phase. In this case, the cross section of the polar part is comparable to that of the aliphatic part, and thus a lamellar structure was expected instead of the Col_h phase (and indeed, a transient lamellar crystalline phase was formed at lower temperatures before the Col_h phase). It appeared that for the lattice parameter $D=49.8$ Å, $V_{mol}=2\ 505$ Å^3 at $T=100$ °C, a slice 4.5 Å thick would contain four molecules. This arrangement did not yield an efficient paving of the lattice (discrepancy between molecular dimensions and columnar cross section). However, the result of the molecular-dynamics calculation suggested that it was preferable to consider a stratum with a thickness of 9.0 Å containing eight molecules to obtain good filling of the available volume. Here, the relative positions of the hydroxy groups are able, through efficient hydrogen-bonding interactions, to ensure the stability of the polar column (see the Supporting Information). The density ratio estimated from MD and XRD analyses for this packing at 100 °C (1.036) shows good agreement with the model (Table 2).

The main driving force for the Col_h formation of **5a** is the importance of the hydrogen-bonding interactions that stabilize the overall architecture, as proven by the modeling. For both **4a** and **5a**, good agreement was observed between the results obtained by using XRD and those found from MD analyses (Table 2). Despite the a priori incompatible molecular conformation, that is, either an inverted triangular shape (**4a**) or quasicylindrical shape (**5a**, quasiequivalence of the two lobes, with a near zero-interfacial curvature), a good segregation in columns was nevertheless achieved between the polar hydroxy parts and the aliphatic parts. For all the compounds, the columns are stabilized by hydrogen-bonding interactions and van der Waals interactions, with the latter then self-organizing into a hexagonal honeycomb packing, that is, a Col_h phase.

Conducting this analysis on **4c** ($D=50.35$ Å, $V_{mol}=1\ 860$ Å^3 at $T=140$ °C) and **5c** ($D=54.15$, $V_{mol}=3\ 150$ Å^3 at $T=100$ °C) led to similar idealized representations. Ten molecules are needed over a thickness of 8.5 Å in the case of **4c**, while for **5c**, eight molecules are necessary to fill a cylinder 9.8 Å thick. MD calculations show a good agreement between molecular and mesophase dimensions, with an almost perfect paving of the two-dimensional lattice. As it can be seen from the MD snapshots (Figure 4 and the Supporting Information), the filling of the available space is more efficient for the two **c** systems, each bearing three and six terminal aliphatic chains, respectively, than for the **a**-system homologues (2 and 4 aliphatic chains), as expected.

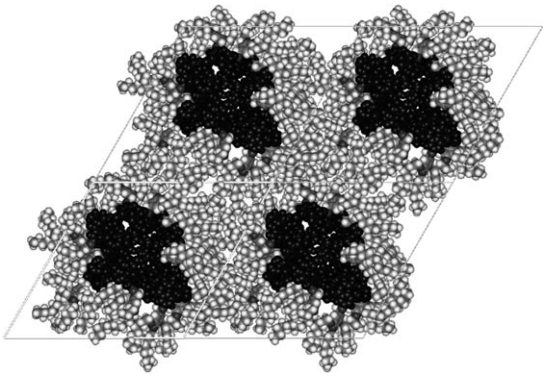

Figure 4. Snapshot of the packing of **4c** after MD in the hexagonal two-dimensional lattice of the Col_h phase (polar column in black).

As for **1c** and **1d**, good packing models in the hexagonal cells were obtained. For **1c** ($D=40.1$ Å, $V_{mol}=1\ 315$ Å^3 at $T=50$ °C), ten molecules can be arranged radially over a thickness of 9.4 Å. For **1d**, with a much larger lattice, 18 molecules over 9.4 Å were necessary ($D=47.1$ Å, $V_{mol}=1\ 010$ Å^3 at $T=60$ °C) to achieve efficient packing. As can be seen from the modeling, the molecules completely occupy the available space (see the Supporting Information).

All the data given above for each compound are summarized in Table 2. It is important to keep in mind that all these molecular models are static and local representations only of a more dynamic and macroscopic reality, however, they are significantly descriptive and useful to explain the supramolecular organization of all these dendrimers within the hexagonal columnar phases. This is why, for instance, the polar cores, in black, do not appear circular but rather distorted in shape instead. Averaging these local arrangements over larger assemblies with random (not correlated) main orientation effectively leads, on the timescale of the experiment, to columns with circular polar cross sections that are compatible with the symmetry of the mesophase.

To access other structural parameters, such as chain area, a convenient way to describe these hexagonal densely packed infinite columns is to locally visualize the distance between columnar hard cores or intercolumnar interfaces by a virtual hexagonal array (honeycomb), embedded within the polar cylindrical-like core (Figure 5). With such a geometrical model (i.e., to consider the column as a hexagonal prism), it is possible to determine the area occupied by one terminal chain on the walls of the Wigner-Seitz cell, and thus to estimate the average conformation of the chains and their degree of squeezing in this arrangement. Indeed, the edge of the hexagonal prism, l, is directly linked to the parameters of the mesophase deduced by using XRD by the relationship $l=D/\sqrt{3}$, and thus the estimation of a specific interfacial area is straightforward. The result of these calculations show acceptable values for the chain area of the dendrimers approaching a tapered shape (i.e., compounds **1c**, **1d**, **2c**, and **5c**) that is, about 40–45 Å^2 (Table 2); in these cases, the chains radiate almost perpendicularly to the interface, and adopt a fanlike conformation and fold as the distance to the interface increases. Discrepancies were found for the chain-deficient compounds such as **4a**, and to a lesser extent for compounds **2a**, **5a**, and **4c**, with chain areas greater than 50 Å^2. To cover the honeycomb interface, the chains, which are not as radially stretched in the plane as for the above compounds, are forced to be tilted in and out of the plane symmetry; this leads to a lesser occupation of the available space, in good agreement with the modeling calculations.

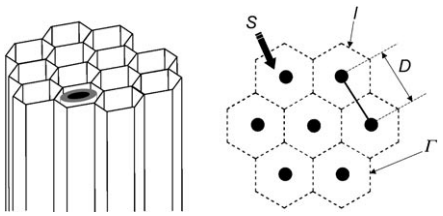

Figure 5. Wigner-Seitz representation of the hexagonal phase (honeycomb array). D is the intercolumnar distance and S, l, and Γ are the surface area, edge, and perimeter of these cells.

Cubic phases, Cub-Im$\bar{3}$m *and Cub*-Pm$\bar{3}$n—*space- filling polyhedral model*: Cubic mesophases are ordered three-dimensional supramolecular edifices that appear optically isotropic when observed between crossed polarizers. Although such phases are routinely observed in lyotropic systems,[43] relatively few thermotropic compounds exhibit cubic phases.[14,17,37c,f,44] Among the dendrimers studied, seven of them were found to self-organize into cubic structures, namely the four compounds of the third generation (**3a**, **3c**, **6a**, and **6c**) bearing linear chains, and the three members of the hexol series of dendrimers bearing peripheral trifurcated chains (**4b**, **5b**, and **6b**). X-ray diffraction analyses enabled us to identify the space groups of the cubic phases, namely, *Im*$\bar{3}$*m* for **6a**, **6c**, **4b**, and **5b** and *Pm*$\bar{3}$*n* for **3a**, and **3c**, the phase symmetry appearing to depend on the size of the polar part.

However, there is no direct evidence whether the phases are bicontinuous or micellar. As discussed previously, their occurrence in the phase sequence along with their molecular structures strongly supports the latter. Indeed, all these dendritic molecules have a very large volume fraction of aliphatic chains in common, and thus a strong interfacial curvature. This forces the dendrimers to deviate from the wedgelike flat shape to adopt a conical conformation with the polar part located at the apex of the conelike structure, despite the important associated entropic cost (conformational limitations). Consequently, based on these molecular conformations and packing considerations, the micellar model appears to be more probable than the bicontinuous one. The former will be considered hereafter as the basis of the molecular organization of these dendrimers, as in the case of the classical dendromesogens[14] and other thermotropic systems showing such phases. Recall that for micellar thermotropic cubic phases, the micelles are necessarily inverted, that is, the polar nucleus of the micelles is embedded in an apolar aliphatic shell.[37]

As for lyotropic micellar cubic phases, their structure results from the ordered three-dimensional packing of micellar aggregates into various cubic symmetries, although, in thermotropic systems, there is no continuous film of solvent separating the micelles.[36,43] Self-organization into such a cubic phase is similar to that described above for the Col_h phase except that in the present case, three-dimensional-like objects are now considered instead of flat, tapered ones. First, the mesogens self-assemble into spheroidlike supramolecular clusters, with this process driven by the amphipathic character of the molecules, as well as steric and energetic constraints. The minimization of the energy cost is achieved by the antiparallel arrangement of the dendrimers to yield a nonpolar micelle. Then, these supramolecular objects subsequently pack into three-dimensional lattices, the stability of the arrangements being controlled by van der Waals interactions and surface-energy minimization (Figure 6). In these molecular edifices, the number of molecules per micelle depends on both the generation and number of terminal chains.

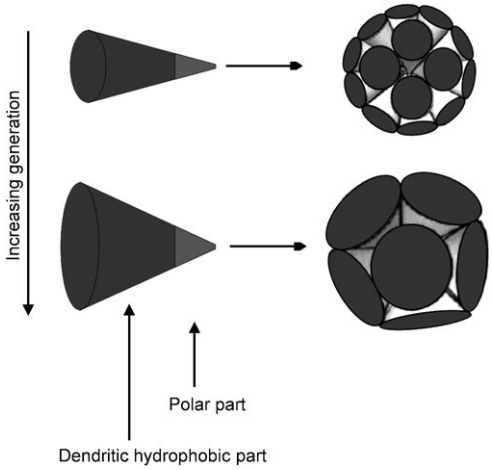

Figure 6. Schematic idealized representation of the self-assembling process of amphiphilic dendrimers into supramolecular clusters. Depending on the aliphatic volume fraction, the size, and thus the number of molecules per micelle, is changed. The height of the dendrimer corresponds approximately to the radius of the micelle.

In the case of the body-centered micellar cubic phase with the $Im\bar{3}m$ space group, the phase consists of the three-dimensional packing of a single type of spherical micelle located at the corners and at the center of the cubic cell. Still under debate,[45] the structure of the $Pm\bar{3}n$ micellar cubic phase is thought to be made of two types of micelles: two quasispherical ones are located at the corners and center of the cubic lattice, and six with a more flattened shape are positioned in the middle of the faces.[46] This latter structure was proposed after the so-called A15[47] structure known in metal alloys (MM'_3) and metal oxides (MO_3). In this case, the atoms M generate a cubic body-centered substructure (i.e., $Im\bar{3}m$ symmetry), and each of the cubic faces contains a pair of the M′ or O atoms located on two of the four tetrahedral sites, leading to breaking up of the symmetry.[48] However, a crystallographic description based on the packing of nondeformable hard spheres seems improper here, as it generates interstices particularly in such noncompact structures. As far as the lyotropic cubic phases are concerned (normal and inverted), these lacunas can be filled by water (normal phase) or hydrocarbon solvents (inverted phase). The overall dynamics of the system allow such a local instantaneous description. In contrast, such a hard-sphere model cannot be applied to cubic thermotropic phases for several reasons. Firstly, because of the excluded volume, which cannot be compensated for in (single component) pure systems made of hard spherical objects, particularly with these two loose-packed cubic lattices. Secondly, unlike metallic ions that interact by means of directional d orbitals to form specific three-dimensional edifices, there are no such preferential bonding directions between spherical micelles, and thus no particular tendency to self-organize according to specific three-dimensional arrangements. Finally, such micelles are not hard like metals or inorganic ions, but have a rather soft shell, and their shape may easily undergo some low-energy elastic deformation favoring area-minimizing structures (surface minimization). All these facts led us to adopt the space-filling polyhedron geometrical model,[27,49] similar to that used in dry soap froths.[50,51] In this description, instead of considering hard and spherical micelles, we looked at the mean distances between the micellar nuclei, which is represented by polyhedral Wigner-Seitz (or Voronoï) cells,[52] the nature and type of which are clearly related to the symmetry of the cubic phase. In these idealized structures, the interior of the polyhedrons is filled by a defined number of dendrimers, the center of gravity being occupied by the polar core (the nucleus), and the end chains lying on the corresponding geometrical surfaces and describing the micellar interface (i.e., films of solvent in lyotropic phases[53]).

Thus, for the $Im\bar{3}m$ phase, the symmetry and the complete filling of the space is achieved if the Wigner-Seitz cell of the body-centered cubic structure, the truncated octahedron (a semiregular Archimedean tetrakaidecahedron formed by eight hexagonal and six square *l*-edge faces), is considered: it is located at the nodes of the cubic lattice ($N_{mic} = (8 \times 1/8) + (1 \times 1) = 2$) (Figure 7a).

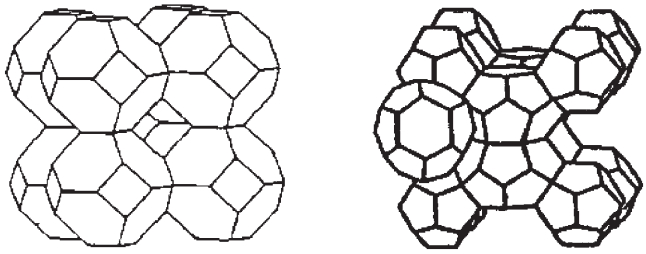

Figure 7. Space-filling polyhedra model. Packing of regular truncated octahedra in the micellar $Im\bar{3}m$ cubic structure (left), and packing of dodecahedra and Goldberg tetradecahedra in the micellar $Pm\bar{3}n$ cubic structure (right).

Concerning the $Pm\bar{3}n$ space group, two polyhedrons must be considered to fill the entire volume and keep the symmetry,[54] namely the regular Platonic dodecahedron (12 pentagonal faces of edge l) located at the center and corners of the cubic cell ($(8\times1/8)+(1\times1)=2$), and the Goldberg tetrakaidecahedron (a semiregular 14-faced polyhedron with two hexagonal faces and 12 pentagonal l-edge faces),[50] occupying two of the four tetrahedral sites of each face of the cubic lattice ($6\times2\times(1/2)=6$) ($N_{mic}=8$) (Figure 7b). From the bond frame formed by mononuclear Si_{46}, Ge_{46}, and Sn_{46} clathrates of type I (A15), which also crystallize in the same $Pm\bar{3}n$ space group, this arrangement of polyhedrons can be recognized (see the Supporting Information).[55] In this non-close-packed lattice, the atoms are arranged in such a way that they form a complicated three-dimensional skeleton through Si–Si bonds by generating an arrangement of two types of polyhedrons, namely, the regular dodecahedron located at the center and corners of the cubic cell and two tetrakaidecahedron on the middle of each face, confirming the appropriate choice of the two polyhedrons.

Table 3. Structural parameters[a] of the cubic phases formed by **6a**, **6c**, **4b**, and **5b** ($Im\bar{3}m$ space group) and by **3a** and **3c** ($Pm\bar{3}n$ space group).

Compd	V_{mol} [Å^3]	a [Å]	l [Å]	S (S') [Å^2]	V (V') [Å^3]	N (N')	N_{Ch} (N'_{Ch})	a_{Ch} (a'_{Ch}) [Å^2]
4b	3 090	54.7	19.34	10 018	81 834	26.5	160.7	62.3
5b	5 505	59.05	20.88	11 674	102 951	18.7	224.4	52.0
6a	4 550	63.3	22.38	13 415	126 818	27.9	223.2	60.15
6c	5 835	66.2	23.40	14 673	145 059	24.9	298.3	49.2
3a	3 960	81.5	18.73	7247 (9071)	50395 (73426)	12.7 (18.55)	101.8 (148.3)	71.2 (61.15)
3c	5 315	82.9	19.05	7 498 (9385)	53 037 (77275)	10.0 (14.55)	120 (174.6)	62.6 (53.8)

[a] V_{mol} = molecular volume at T, the temperature of the X-ray experiment; a = lattice parameter of the cubic phase; V = volume of the regular polyhedron (the truncated octahedron for the $Im\bar{3}m$ cubic phase or the dodecahedron for the $Pm\bar{3}n$ cubic phase); V' = volume of the Goldberg tetrakaidecahedron ($Pm\bar{3}n$ cubic phase); S = surface of the regular polyhedron; S' = surface of the semiregular tetrakaidecahedron; l = edge of the polyhedron. Geometrical parameters: $a=2\sqrt{2}l$, $S=(12\sqrt{3}+6)l^2$, $V=8\sqrt{2}l^3$ for the $Im\bar{3}m$, and $a=\frac{1}{2}(2\sqrt{3}+3+\sqrt{5})l$, $S=3\sqrt{(25+10\sqrt{5})}l^2$, $V=\frac{1}{4}(15+7\sqrt{5})l^3$ for the $Pm\bar{3}n$ cubic phase, $S'=S+3\sqrt{3}l^2$, $V'=\frac{1}{6}(a^3-2V)$. $N(N')$ = number of aggregation in the regular (irregular) polyhedron ($N(N')=V\ (V')/V_{mol}$). N_{Ch} (N'_{Ch}) = number of chains per micelle. a_{Ch}/a'_{Ch} = chain area $a_{Ch}/a'_{Ch}=S(S')/N(N')$.

This concept is of particular interest,[27] as the judicious choice of the elementary polyhedron (each point of its surface represents the mean distance between adjacent micellar nuclei and by extrapolation can be seen as the micellar interface) in the corresponding cubic structure, or other three-dimensional structures,[27,56] will allow for the complete filling of the volume. It can thus be adapted to the description of the pure, inverted thermotropic micellar cubic phases under study. This geometrical analogy also offers easier access to molecular and micellar characteristics as a function of the cubic mesophase lattice parameter, because the volume and surface area of the polyhedrons are determined mathematically, and the lattice parameter (a) and the edge of the polyhedron (l) are geometrically linked (see below). Note that for the $Pm\bar{3}n$ case, despite the fact that these two polyhedrons are only slightly distorted, the relationships between a and l still remain valid.[57] The knowledge of l will give access to the interface and the chain cross-sectional area, and should permit a better understanding between molecular structure and cubic space group.

The relationship linking a and l allows the volumes (and the surfaces) of the various polyhedral micelles to be determined (Table 3) and compared: those forming the $Pm\bar{3}n$ lattice are approximately 35–60% smaller than those forming the $Im\bar{3}m$ lattice (for identical dendritic arborescence, the difference is the size of the polar head) and consequently a smaller number of dendrimers self-assemble in the former than in the latter. It also permits access to the chain-area values at the interface of the polyhedrons. Indeed, as for the hexagonal phases described above, it is also possible to evaluate the surface area of the aliphatic chains and thus their degree of order (orientation, squeezing) at the micellar interface (with the number of chains per micelle and the surface area of the micelles known). It is immediately apparent, and expected, that the chain area is greater in the cubic phases (Table 3) than in the Col_h phase (Table 2). The greater area is a consequence of the molecular shape change from flat and tapered to conelike and therefore, in the cubic phase, the chains radiate isotropically with respect to the spheroid micellar nucleus.

For similar dendritic topologies (**3a** and **6a**, and **3c** and **6c**, respectively), the chain area is, on average, smaller for compounds of type **6** than for those of type **3**. This can be understood as the two hexols (**6a** and **6c**) have a larger polar lobe than the corresponding triols (**3a** and **3c**), and thus preferably adopt an overall conformation close to that of a truncated cone rather than a true conical one. This results in the supramolecular aggregation of the hexols into larger micelles, with a smaller interfacial curvature than those of the triols. In this case, the chain area is minimized (ca. 50–60 Å^2), and so is the interfacial area between neighboring micelles (minimization of the surface free energy). Consequently, the smaller the chain area is (denser chain packing), the smaller the interfacial curvature is, and the larger the micelle is. Moreover, adding chains but maintaining the dendritic and polar parts constant (**a**→**c**) also leads to a denser packing of the chains, which confirms the above assumption, and leads to a lowering of the free energy of the system. The dendrimers bearing trifurcated chains (**4b** and **5b**) also have a truncated cone shape and a similar chain-area value, and behave like **6**. The interfacial area decreases with the generation or with the number of peripheral chains (**a**→**c**) (Table 3).

This is in contrast with the two triols of the third generation (**3a** and **3c**), which self-assemble into the $Pm\bar{3}n$ cubic phase. Here, the polar head is small compared with that of **6a** and **6c** and the overall molecular conformation is assumed in a first approximation to be close to a cone shape.

Therefore, the tendency to self-assemble into smaller micelles is enhanced (Table 3). However, considering the two-micelle model, these small micelles should possess a larger free energy than those formed by **6**. This is a direct consequence of the rather large chain area calculated at the micellar "interface" (Table 3, 60–70 $Å^2$; 10 $Å^2$ more than in the $Im\bar{3}m$ case), implying more disordered chains (note that the chain area is smaller for the larger micelles of the primitive cubic cell than for the smaller ones). This unfavorable gain of entropy (with respect to **6**) would lead to an increase of the free energy of the small micelles. A way to compensate for this entropy excess would consist of the self-assembling process of two different types of micelles in equilibrium, that is, two small and nearly spherical ones and six larger and flattened ones as in the $Pm\bar{3}n$ structure, in agreement with the breaking of symmetry. Thus, a more satisfactory model may be needed (the larger micelles should absorb the smaller ones!), as this $Pm\bar{3}\bar{3}n$ structure still remains a thermodynamically stable mesophase. A more stable and suitable model would be that proposed by Kamien,[58] which considers columns in the cubic lattice formed by the face-to-face fusion of consecutive Goldberg tetrakaidecahedrons through their hexagonal faces. Indeed, the $Pm\bar{3}\bar{3}n$ cell can be described differently: the unit cell includes eight sites, which can be subdivided into three pairs of columnar sites evenly spaced along the bisectors of the cubic cell faces and two interstitial sites at the center and corners of the cubic lattice (Figure 8), occupying approximately 80 and 20% of

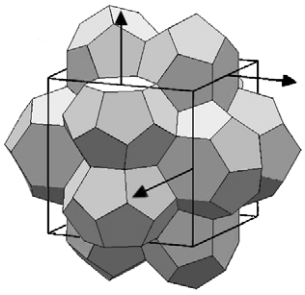

Figure 8. Schematic representation of the three-dimensional interlocking pinched columns model lattice. The arrows indicate the growth direction of the evenly pinched columns.

the volume, respectively. The columns resulting from the fusion of the tetrakaidecahedron form a set of mutually perpendicular and interlocking columns (Figure 8), in a way similar to the representation of the cubic blue phase BPII;[59] though here the columns are not double-twisted, but evenly pinched. The interstitial space left at the junctions between three columns corresponds to a regular dodecahedron and can be entirely or partially filled. In the case of empty interstices, the excluded volume represents 18.6% of the entire cell corresponding to approximately 26 and 20 molecular volume equivalents (for the two interstices) out of 137 (**3a**) and 107 (**3c**) molecules, respectively. In this case, the new calculated chain-surface areas amount to 39.75 and 35.0 $Å^2$ for **3a** and **3c**, respectively, in the most extreme (improbable) empty interstices situation, whereas larger values are obtained when they are totally filled (48.85 and 42.95 $Å^2$ for **3a** and **3c**, respectively). These new values of the chain areas, close to those found in the Col_h phases, are indicative of a denser packing and thus of more stable systems. Due to the energy cost involved, the case of an unfilled interstice is highly improbable, and thus diffusion of molecules from the pinched columns into the interstice likely occurs instead, resulting in some local distortions or undulations of the columns. This led us to wonder whether the conical shape of the dendrimers is a necessary requirement for them to self-assemble into the $Pm\bar{3}n$ cubic phase, the restriction of molecular conformations contributing to an increase of the entropy of the system. On the basis of the present results, such a molecular conformation is truly not an essential condition for the formation of evenly pinched columns, 3×3 interlocked into a three-dimensional network.

As for the hexagonal systems, the static and local description given here does not reflect the entire reality of these mesophases, but gives us a fairly good account of the molecular packing of these dendrimers at the local scale. For the same reasons, and for the $Im\bar{3}m$ cubic phase, it is easy to conceive that due to thermal motion all the truncated octahedrons are close to perfect spheres that fully fill the available space. The situation is slightly more delicate as far as the interlocking, evenly pinched column model for the $Pm\bar{3}\bar{3}n$ cubic phase is concerned. It is very likely that the pinched columns are not frozen, and move along the three directions of space (parallel to their main columnar axis), in such a way that a time–average filling of the space is apparent, that is, diffusion of molecules likely occurs, which corresponds to the filling of the interstices.

Conclusion

A detailed systematic study on Janus amphiphilic block codendrimers was carried out. The generation of both dendritic lobes and the number of peripheral aliphatic chains were modified independently, allowing for insight into some structure–property relationships. Increasing the generation and/or the number of chains leads to a stepwise increase of the dendritic–aliphatic interface, and to the formation of columnar and cubic phases accordingly. The control of the hydrogen-bonding ability by tuning the polar lobe size was reflected by the strong stabilization, and in some cases modification, of the mesophases. For example, decomposition was reached before clearing into the isotropic liquid phases in some cases. Models of these supramolecularly organized constructions were proposed. The packing of these new codendrimers into hexagonal columnar phases was understood with the help of molecular dynamics. Important structural parameters could be extracted and this allowed a direct correlation between both the molecular and mesostructural dimensions. As for the cubic phases, the geometrical space-filling polyhedron model was successfully applied here. The use of the single elementary Wigner-Seitz cell of the bcc lat-

tice was sufficient to explain the molecular organization within the $Im\bar{3}m$ cubic phase. It was demonstrated, on the contrary, that the most satisfactory explanation of the molecular organization of the dendrimers with the $Pm\bar{3}n$ lattice consists of the formation of an infinite three-dimensional interlocking network of evenly pinched columns. This study also showed that the formation of columnar and cubic phases is not restricted to flat, tapered, conical molecular conformations, but that new structural criteria may be applied for the design of liquid-crystalline dendrimers.

The amphiphilic nature of the dendrimers resembles surfactant properties, and indeed preliminary investigations showed that they all exhibited a strong tendency to form films at the air/water interface. These results will be reported in due course.

Acknowledgements

I.B. would like to thank the European Union for support and funding through the RTN project "Supramolecular Liquid Crystal Dendrimers (LCDD)" and Miss Marylin Gleyzes, who was involved in part of this work through a six-month training course. The CNRS and the University Louis Pasteur Strasbourg (UMR 7504) are also greatly acknowledged for their constant help and financial support. Many thanks to Pr. Yves Galerne (GMO-IPCMS) for useful discussions and interesting and pertinent comments while reading the manuscript.

[1] D. A. Tomalia, *Mater. Today* **2005**, 34–46.

[2] a) D. A. Tomalia, A. M. Naylor, W. A. Goddard III, *Angew. Chem.* **1990**, *102*, 119–157; *Angew. Chem. Int. Ed. Engl.* **1990**, *29*, 138–175; b) D. A. Tomalia, H. Dupont Durst, *Top. Curr. Chem.* **1993**, *165*, 193–313; c) J. Issberner, R. Moors, F. Vögtle, *Angew. Chem.* **1994**, *106*, 2507–2514; *Angew. Chem. Int. Ed. Engl.* **1994**, *33*, 2413–2420; d) N. Ardoin, D. Astruc, *Bull. Soc. Chim. Fr.* **1995**, *132*, 875–909; e) B. I. Voit, *Acta Poly.* **1995**, *46*, 87–99; f) G. R. Newkome, C. N. Moorefield, F. Vögtle in *Comprehensive Supramolecular Chemistry, Vol. 10* (Eds.: J. L. Atwood, J. E. D. Davies, D. D. MacNicol, F. Vögtle, J.-M. Lehn), Pergamon, Oxford, **1996**, pp. 777–832; g) P. R. Ashton, S. E. Boyd, C. L. Brown, S. A. Nepogodiev, E. W. Meijer, H. W. I. Peerlings, J. F. Stoddart, *Chem. Eur. J.* **1997**, *3*, 974–984; h) F. Zeng, S. C. Zimmerman, *Chem. Rev.* **1997**, *97*, 1681–1712; i) O. A. Matthews, A. N. Shipway, J. F. Stoddart, *Prog. Polym. Sci.* **1998**, *23*, 1–56; j) H. F. Chow, T. K. K. Mong, M. F. Nongrum, C. W. Wan, *Tetrahedron* **1998**, *54*, 8543–8660; k) M. Fischer, F. Vögtle, *Angew. Chem.* **1999**, *111*, 934–955; *Angew. Chem. Int. Ed.* **1999**, *38*, 884–905; l) C. J. Hawker, *Adv. Polym. Sci.* **1999**, *147*, 113–160; m) K. Inoue, *Prog. Polym. Sci.* **2000**, *25*, 453–571; n) F. Vögtle, S. Gestermann, R. Hesse, H. Schwierz, B. Windisch, *Prog. Polym. Sci.* **2000**, *25*, 987–1041; o) I. P. Beletskaya, A. V. Chuchurjukin, *Russ. Chem. Rev.* **2000**, *99*, 639–660; p) G. R. Newkome, C. N. Moorefield, F. Vögtle, *Dendrimers and Dendrons: Concepts, Synthesis and Applications*, VCH, Weinheim, **2001**.

[3] See the special issues dedicated to dendrimers: a) *Top. Curr. Chem.* **1998**, *197*, 1–228; b) *Top. Curr. Chem.* **2000**, *210*, 1–308; c) *Top. Curr. Chem.* **2001**, *212*, 1–194; d) *Top. Curr. Chem.* **2001**, *217*, 1–238; e) *Top. Curr. Chem.* **2003**, *228*, 1–237; f) *C. R. Chim.* **2003**, *6*, 709–1212; g) *Prog. Polym. Sci.* **2005**, *30*, 217–505; h) *Adv. Drug Delivery Rev.* **2005**, *57*, 2101–2286.

[4] a) A. W. Bosman, H. M. Janssen, E. W. Meijer, *Chem. Rev.* **1999**, *99*, 1665–1688; b) D. C. Tully, J. M. J. Fréchet, *Chem. Commun.* **2001**, 1229–1239; c) B. Dong, F. Huo, L. Zhang, X. Yang, Z. Wang, X. Zhang, S. Gong, J. Li, *Chem. Eur. J.* **2003**, *9*, 2331–2336; d) L. Merz, H.-J. Günterodt, L. J. Scherer, E. C. Constable, C. E. Housecroft, M. Neuburger, B. A. Hermann, *Chem. Eur. J.* **2005**, *11*, 2307–2318; e) B. A. Hermann, L. J. Scherer, C. E. Housecroft, E. C. Constable, *Adv. Funct. Mater.* **2006**, *16*, 221–235.

[5] a) H. Frey, C. Lach, K. Lorenz, *Adv. Mater.* **1998**, *10*, 279–293; b) C. Gorman, *Adv. Mater.* **1998**, *10*, 295–309; c) J. Roovers, B. Comanita, *Adv. Polym. Sci.* **1999**, *142*, 179–228; d) J.-P. Majoral, A.-M. Caminade, *Chem. Rev.* **1999**, *99*, 845–880; e) G. R. Newkome, E. He, C. N. Moorefield, *Chem. Rev.* **1999**, *99*, 1689–1746; f) I. Cuadrado, M. Moran, C. M. Casado, B. Alonso, J. Losada, *Coord. Chem. Rev.* **1999**, *193–195*, 395–445; g) A.-M. Caminade, A. Maraval, J.-P. Majoral, *Eur. J. Inorg. Chem.* **2006**, 887–901.

[6] a) D. Astruc, *C. R. Acad. Sci. Ser. II* **1996**, 322, 757–766; b) D. K. Smith, F. Diederich, *Chem. Eur. J.* **1998**, *4*, 1353–1361; c) G. M. Dykes, *J. Chem. Technol. Biotechnol.* **2001**, *76*, 903–918; d) R. Esfand, D. A. Tomalia, *Drug Discovery Today* **2001**, *6*, 427–436; e) S. Hecht, J. M. J. Fréchet, *Angew. Chem.* **2001**, *113*, 76–94; *Angew. Chem. Int. Ed.* **2001**, *40*, 74–91; f) M. J. Cloninger, *Curr. Opin. Chem. Biol.* **2002**, *6*, 742–748; g) F. Aulenta, W. Hayes, S. Rannard, *Eur. Polym. J.* **2003**, *39*, 1741–1771; h) U. Boas, M. H. Heegaard, *Chem. Soc. Rev.* **2004**, *33*, 43–63; i) D. Paul, H. Miyake, S. Shinoda, H. Tsukube, *Chem. Eur. J.* **2006**, *12*, 1328–1338.

[7] S. M. Grayson, J. M. J. Fréchet, *Chem. Rev.* **2001**, *101*, 3819–3867.

[8] D. A. Tomalia, *Adv. Mater.* **1994**, *6*, 529–539.

[9] P. G. de Gennes, H. Hervet, *J. Phys. Lett.* **1983**, *44*, 351–360.

[10] a) S. A. Ponomarenko, N. I. Boiko, V. P. Shibaev, *Polym. Sci. Part C* **2001**, *43*, 1–45 (Vysokomol. Soed. Ser. C **2001**, 43, 1601–1650); b) D. Guillon, R. Deschenaux, *Curr. Opin. Solid State Mater. Sci.* **2002**, *6*, 515–525; c) B. Donnio, D. Guillon, Adv. *Polym. Sci.* **2006**, *201*, 45–155.

[11] a) V. Percec, C. G. Cho, C. Pugh, D. Tomazos, *Macromolecules* **1992**, *25*, 1164–1176; b) V. Percec, M. Kawasumi, *Macromolecules* **1992**, *25*, 3843–3850; c) S. Bauer, H. Fischer, H. Ringsdorf, *Angew. Chem.* **1993**, *105*, 1658–1661; *Angew. Chem. Int. Ed. Engl.* **1993**, *32*, 1589–1592; d) V. Percec, P. Chu, M. Kawasumi, *Macromolecules* **1994**, *27*, 4441–4453; e) S. W. Hanh, S. Y. K. Yun, J. I. Jin, O. H. Han, *Macromolecules* **1998**, *31*, 6417–6425; f) A. Sunder, M. F. Quincy, R. Mülhaupt, H. Frey, *Angew. Chem.* **1999**, *111*, 3107–3110; *Angew. Chem. Int. Ed.* **1999**, *38*, 2928–2930.

[12] P. J. Flory, *Principles of Polymer Chemistry*, Cornell University Press, Ithaca (NY), **1953**.

[13] a) Y. H. Kim, *J. Polym. Sci. Part A* **1998**, *36*, 1685–1698; b) H. Frey, D. Hölter, *Acta Polym.* **1999**, *50*, 67–76; c) A. Hult, M. Johansson, E. Malmström, *Adv. Polym. Sci.* **1999**, *143*, 1–34.

[14] a) S. D. Hudson, H. T. Jung, V. Percec, W. D. Cho, G. Johansson, G. Ungar, V. S. K. Balagurusamy, *Science* **1997**, *278*, 449–452; b) V. S. K. Balagurusamy, G. Ungar, V. Percec, G. Johansson, *J. Am. Chem. Soc.* **1997**, *119*, 1539–1555; c) V. Percec, W. D. Cho, P. E. Mosier, G. Ungar, D. J. P. Yeardley, *J. Am. Chem. Soc.* **1998**, *120*, 11061–11070; d) G. Ungar, V. Percec, M. N. Holerca, G. Johansson, J. A. Heck, *Chem. Eur. J.* **2000**, *6*, 1258–1266; e) V. Percec, W. D. Cho, G. Ungar, D. J. P. Yeardley, *Angew. Chem.* **2000**, *112*, 1661–1666; *Angew. Chem. Int. Ed.* **2000**, *39*, 1597–1602; f) V. Percec, W. D. Cho, M. Möller, S. A. Prokhorova, G. Ungar, D. J. P. Yeardley, *J. Am. Chem. Soc.* **2000**, *122*, 4249–4250; g) V. Percec, W. D. Cho, G. Ungar, *J. Am. Chem. Soc.* **2000**, *122*, 10273–10281; h) V. Percec, W. D. Cho, G. Ungar, D. J. P. Yeardley, *J. Am. Chem. Soc.* **2001**, *123*, 1302–1315; i) V. Percec, M. Glodde, T. K. Bera, Y. Miura, I. Shiyanovskaya, K. D. Singer, V. S. K. Balagurusamy, P. A. Heiney, I. Schnell, A. Rapp, H.-W. Spiess, S. D. Hudson, H. Duan, *Nature* **2002**, *419*, 384–387; j) G. Ungar, Y. Liu, X. Zeng, V. Percec, W. D. Cho, *Science* **2003**, *299*, 1208–1211; k) X. Zeng, G. Ungar, Y. Liu, V. Percec, A. E. Dulcey, J. K. Hobbs, *Nature* **2004**, *428*, 157–160; l) V. Percec, A. E. Dulcey, V. S. K. Balagurusamy, Y. Miura, J. Smidrkal, M. Peterca1, S. Nummelin, U. Edlund, S. D. Hudson, P. A. Heiney, H. Duan, S. N. Magonov, S. A. Vinogradov, *Nature* **2004**, *430*, 764–768; m) V. Percec, C. M. Mitchell, W.-D. Cho, S. Uchida, M. Glodde, G. Ungar, X. Zeng, Y. Liu, V. S. K. Balagurusamy, P. A. Heiney, *J. Am. Chem. Soc.* **2004**, *126*, 6078–6094; n) V. Percec, M. Peterca,

M. J. Sienkowska, M. A. Ilies, E. Aqad, J. Smidrkal, P. A. Heiney, *J. Am. Chem. Soc.* **2006**, *128*, 3324–3334.
[15] a) D. J. Pesak, J. S. Moore, *Angew. Chem.* **1997**, *109*, 1709–1712; *Angew. Chem. Int. Ed. Engl.* **1997**, *36*, 1636–1639; b) H. Meier, M. Lehmann, U. Kolb, *Chem. Eur. J.* **2000**, *6*, 2462–2469.
[16] a) B. Dardel, D. Guillon, B. Heinrich, R. Deschenaux, *J. Mater. Chem.* **2001**, *11*, 2814–2831; b) S. Campidelli, J. Lenoble, J. Barberá, F. Paolucci, M. Marcaccio, D. Paolucci, R. Deschenaux, *Macromolecules* **2005**, *38*, 7915–7925.
[17] a) V. Percec, P. Chu, G. Ungar, J. Zhou, *J. Am. Chem. Soc.* **1995**, *117*, 11441–11454; b) J. L. Li, K. A. Crandall, P. Chu, V. Percec, R. G. Petschek, C. Rosenblatt, *Macromolecules* **1996**, *29*, 7813–7819.
[18] a) L. Gehringer, D. Guillon, B. Donnio, *Macromolecules* **2003**, *36*, 5593–5601; b) L. Gehringer, C. Bourgogne, D. Guillon, B. Donnio, *J. Am. Chem. Soc.* **2004**, *126*, 3856–3867.
[19] J. Barberá, B. Donnio, L. Gehringer, D. Guillon, M. Marcos, A. Omenat, J. L. Serrano, *J. Mater. Chem.* **2005**, *15*, 4093–4105.
[20] C. J. Hawker, K. L. Wooley, J. M. J. Fréchet, *J. Chem. Soc. Perkin Trans. 1* **1993**, 1287–1297.
[21] D. J. Pesak, J. S. Moore, *Tetrahedron* **1997**, *53*, 15331–15347.
[22] K. Aoi, K. Itoh, M. Okada, *Macromolecules* **1997**, *30*, 8072–8074.
[23] a) Y. Pan, W. T. Ford, *Macromolecules* **1999**, *32*, 5468–5470; b) Y. Pan, W. T. Ford, *Macromolecules* **2000**, *33*, 3731–3738.
[24] a) T. Imae, M. Ito, K. Aoi, K. Tsutsumiuchi, H. Noda, M. Okada, *Colloids Surf. A* **2000**, *175*, 225–234; b) M. Ito, T. Imae, K. Aoi, K. Tsutsumiuchi, H. Noda, M. Okada, *Langmuir* **2002**, *18*, 9757–9764; c) K. Tanaka, S. Dai, T. Kajiyama, K. Aoi, M. Okada, *Langmuir* **2003**, *19*, 1196–1202.
[25] a) J. Ropponen, S. Nummelin, K. Rissanen, *Org. Lett.* **2004**, *6*, 2495–2497; b) N. R. Luman, M. W. Grinstaff, *Org. Lett.* **2005**, *7*, 4863–4866; c) H.-F. Chow, K.-F. Ng, Z.-Y. Wang, C.-H. Wong, T. Luk, C.-M. Lo, Y.-Y. Yang, *Org. Lett.* **2006**, *8*, 471–474.
[26] a) I. M. Saez, J. W. Goodby, *J. Mater. Chem.* **2005**, *15*, 26–40; b) V. Percec, M. R. Imam, T. K. Bera, V. S. K. Balagurusamy, M. Peterca, P. A. Heiney, *Angew. Chem.* **2005**, *117*, 6674–6679; *Angew. Chem. Int. Ed.* **2005**, *44*, 4739–4745.
[27] G. Ungar, X. Zeng, *Soft Matter* **2005**, *1*, 95–106.
[28] a) J. Kohda, K. Shinozuka, H. Sawai, *Tetrahedron Lett.* **1995**, *36*, 5575–5578; b) F. Caturla, J. Enjo, M. C. Bernabeu, S. Le Serre, *Tetrahedron* **2004**, *60*, 1903–1911; c) F. Otis, N. Voyer, A. Polidori, B. Pucci, *New J. Chem.* **2006**, *30*, 185–190.
[29] M. Ueda, A. Kameyama, K. Hashimoto, *Macromolecules* **1988**, *21*, 19–24.
[30] a) R. M. Nouguier, M. Mchich, *J. Org. Chem.* **1985**, *50*, 3296–3298; b) R. M. Nouguier, M. Mchich, *J. Org. Chem.* **1987**, *52*, 2995–2997.
[31] O. Mitsunobu, *Synthesis* **1981**, 1–28.
[32] J. Malthête, H. T. Nguyen, C. Destrade, *Liq. Cryst.* **1993**, *13*, 171–187.
[33] a) P. Sotta, *J. Phys. II* **1991**, *1*, 763–772; b) P. Sakya, J. M. Seddon, R. H. Templer, *J. Phys. II* **1994**, *4*, 1311–1331; c) M. Impéror-Clerc, M. Veber, A. M. Levelut, *ChemPhysChem* **2001**, *2*, 533–535.
[34] In lyotropic systems, the following convention is used and has been kept here: mesophases with a normal topology, for example, oil-in-water phases are said to possess a positive curvature with the polar parts pointing outwards and the apolar parts inwards, in contrast to inverted mesophases (opposite topology for example, water-in-oil phases), which thus have a negative curvature.
[35] a) R. Vargas, P. Mariani, A. Gulik, V. Luzzati, *J. Mol. Biol.* **1992**, *225*, 137–145; b) H. Delacroix, T. Gulik-Krzywicki, P. Mariani V. Luzzati, *J. Mol. Biol.* **1993**, *229*, 526–539; c) T. Gulik-Krzywicki, H. Delacroix, *Biol. Cell* **1994**, *80*, 193–201; d) A. Gulik, H. Delacroix, G. Kirschner, V. Luzzati, *J. Phys. II* **1995**, *5*, 445–464; e) M. Clerc, *J. Phys. II* **1996**, *6*, 961–968.
[36] a) K. Fontell, *Colloid Polym. Sci.* **1990**, *268*, 264–295; b) S. T. Hyde in *Handbook of Applied Surface and Colloid Chemistry* (Ed.: K. Holmberg), Wiley, **2001**, pp. 299–322; c) P. Sakya, J. M. Seddon, R. H. Templer, R. J. Mirkin, G. J. T. Tiddy, *Langmuir* **1997**, *13*, 3706–3714.
[37] a) K. Borisch, S. Diele, P. Göring, H. Kresse, C. Tschierske, *Angew. Chem.* **1997**, *109*, 2188–2190; *Angew. Chem. Int. Ed. Engl.* **1997**, *36*, 2087–2089; b) S. Diele, P. Göring in *Handbook of Liquid Crystals, Vol. 2B* (Eds.: D. Demus, J. W. Goodby, G. W. Gray, H. W. Spiess, V. Vill), Wiley, Weinheim, **1998**, pp. 887–900; c) S. D. Hudson, H. T. Jung, P. Kewsuwan, V. Percec, W. D. Cho, *Liq. Cryst.* **1999**, *26*, 1493–1499; d) X. H. Cheng, S. Diele, C. Tschierske, *Angew. Chem.* **2000**, *112*, 605–608; *Angew. Chem. Int. Ed.* **2000**, *39*, 592–595; e) S. Diele, *Curr. Opin. Colloid Interface Sci.* **2002**, *7*, 333–342; f) T. Kato, T. Matsuoka, M. Nishii, K. Kamikawa, K. Kanie, T. Nishimura, E. Yashima, S. Ujiie, *Angew. Chem.* **2004**, *116*, 2003–2006; *Angew. Chem. Int. Ed.* **2004**, *43*, 1969–1972; g) B. K. Cho, A. Jain, S. M. Gruner, U. Wiesner, *Science* **2004**, *305*, 1598–1601.
[38] This compound was reported to exhibit an additional mesophase, which was not detected in our case (Cr 63 Col_h 64 Cub-$Pm\bar{3}n$ 87 I): K. Borisch, S. Diele, P. Göring, H. Kresse, C. Tschierske, *J. Mater. Chem.* **1998**, *8*, 529–543. However, it appeared that the occurrence of the cubic mesophase and the transition temperatures strongly depend on contamination by small amounts of water. Thus, the phase sequence of the completely dried sample is Cr 48 Col_h 65 Cub-$Pm\bar{3}n$ 78 I, whereas, after the work-up procedure, the phase sequence is similar to ours reported here, that is, Cr 62 Col_h 75 I: R. Dunkel, M. Hahn, K. Borisch, B. Neumann, H. H. Rüttinger, C. Tschierske, *Liq. Cryst.* **1998**, *24*, 211–213.
[39] a) K. Borisch, S. Diele, P. Göring, H. Müller, C. Tschierske, *Liq. Cryst.* **1997**, *22*, 427–443; b) K. Borisch, S. Diele, P. Göring, H. Kresse, C. Tschierske, *J. Mater. Chem.* **1998**, *8*, 529–543; c) A. Pegenau, T. Hegmann, C. Tschierske, S. Diele, *Chem. Eur. J.* **1999**, *5*, 1643–1660.
[40] J. M. Seddon, *Biochim. Biophys. Acta* **1990**, *1031*, 1–69.
[41] a) H. Ringsdorf, B. Schlarb, J. Venzmer, *Angew. Chem.* **1988**, *100*, 117–162; *Angew. Chem. Int. Ed. Engl.* **1988**, *27*, 113–158; b) C. Tschierske, *Prog. Polym. Sci.* **1996**, *21*, 775–852.
[42] a) K. Borisch, C. Tschierske, P. Göring, S. Diele, *Chem. Commun.* **1998**, 2711–2712; b) S. Fischer, H. Fischer, S. Diele, G. Pelzl, K. Jankowski, R. R. Schmidt, V. Vill, *Liq. Cryst.* **1994**, *17*, 855–861.
[43] a) J. M. Seddon, R. H. Templer, *Philos. Trans. R. Soc. London Ser. A* **1993**, *344*, 377–401; b) J. M. Seddon, R. H. Templer in *Handbook of Biological Physics, Vol. 1* (Eds.: R. Lipowsky, E. Sackmann), Elsevier, Leiden, The Netherlands, **1995**, pp. 97–160.
[44] a) S. Kutsumizu, *Curr. Opin. Colloid Interface Sci.* **2002**, *7*, 537–543; b) M. Impéror-Clerc, *Curr. Opin. Chem. Biol.* **2005**, *9*, 370–376.
[45] a) A. Tardieu, V. Luzzati, *Biochim. Biophys. Acta* **1970**, *219*, 11; b) K. Fontel, K. K. Fox, E. Hanson, *Mol. Cryst. Liq. Cryst. Lett.* **1985**, *1*, 9.
[46] a) R. Vargas, P. Mariani, A. Gulik, V. Luzzati, *J. Mol. Biol.* **1992**, *225*, 137–145; b) V. Luzzati, R. Vargas, P. Mariani, A. Gulik, H. Delacroix, *J. Mol. Biol.* **1993**, *229*, 540–551; c) A. Gulik, H. Delacroix, G. Kirschner, V. Luzzati, *J. Phys. II* **1995**, *5*, 445–464; d) V. Luzzati, *J. Phys. II* **1995**, *5*, 1649–1669.
[47] G. Hägg, N. Schönberg, *Acta Crystallogr.* **1954**, *7*, 351–352.
[48] M. R. Fitzsimmons, J. A. Eastment, R. A. Robinson, A. C. Lawson, J. D. Thompson, R. Movshovitch, J. Satti, *Phys. Rev. B* **1993**, *48*, 8245–8252.
[49] M. O'Keeffe, *Acta Crystallogr. Sect. A* **1998**, *54*, 320–329.
[50] a) D. Weaire, R. Phelan, *Philos. Mag. Lett.* **1994**, *69*, 107–110; b) D. Weaire, *The Kelvin Problem*, Taylor & Francis, London, **1996**; c) T. Aste, D. Weaire, *The Pursuit of Perfect Packing*, Institute of Physics Publishing, Bristol and Philadelphia, **2000**; d) A. Bölcskei, *Period. Polytech. Mech. Eng.* **2003**, *47*, 15–23.
[51] a) J.-F. Sadoc, N. Rivier, *Foams and Emulsions*, Kluwer, Dordrecht, The Netherlands, **1999**; b) S. Hilgenfeldt, *Nieuw Archief voor Wiskunde*, **2002**, *5*, 224–230.
[52] A. K. van der Vegt, "Order in space", to be found under http://www.vssd.nl/hlf, **2001**.
[53] J. Charvolin, *Contemp. Phys.* **1990**, *31*, 1–17.
[54] J. Charvolin, J.-F. Sadoc, *J. Phys.* **1988**, *49*, 521–526.

[55] a) G. B. Adams, M. Keeffe, A. A. Demkov, O. F. Sankey, Y.-M. Huang, *Phys. Rev. B* **1994**, *49*, 8048–8053; b) C. A. Perottoni, J. A. H. da Jornada, *J. Phys. Condens. Matter* **2001**, *13*, 5981–5998.
[56] G. Ungar, Y. Liu, X. Zeng, V. Percec, W. D. Cho, *Science* **2003**, *299*, 1208–1211.
[57] J.-F. Sadoc, R. Mosseri, *Frustration Géométrique*, Eyrolles, Paris, **1997**.
[58] a) P. Ziherl, R. D. Kamien, *Phys. Rev. Lett.* **2000**, *85*, 3528–3531; b) P. Ziherl, R. D. Kamien, *J. Phys. Chem. B* **2001**, *105*, 10147–10158.
[59] a) D. C. Wright, N. D. Mermin, *Rev. Mod. Phys.* **1989**, *61*, 385–432; b) P. P. Crooker, *Liq. Cryst.* **1989**, *5*, 751–775.

Received: March 31, 2006
Published online: August 7, 2006

